AN ABSTRACT OF THE THESIS OF

Chun-Chia Hsu for the degree of Master of Science in Mechanical Engineering presented on December 3, 1991.

Title: Range of Motion of Beetle Body as a Function of Leg Parameters

Redacted for Privacy

Abstract approved:_____
Eugene F. Fichter

This thesis examines the influence on range-of-motion of beetle body of changes in leg segment parameters. From beetle's leg orientation, influence of the following leg segment parameters are investigated: coxa length, coxa twist and body-coxa joint.

Kinematic equations are derived for legs of the beetle. Roots of quartic polynomials obtained while solving the kinematic equations are found by using the Bairstow (1966) numerical method. Inverse kinematic solutions are obtained for each leg and used to determine whether a point is within the body range of motion or not. An algorithm developed by Mason (1957) and Cordray (1957) for tracing closed boundaries is used to find

ranges of motion of the body and feet.

Changes in body range of motion caused by alteration in leg segment parameters are complex and not easy to explain. Similarities between changes in body range of motion and foot range of motion are observed. A great deal more work is necessary to fully understand the importance of observed changes.

Range of Motion of Beetle Body as a Function of Leg Parameters

by

Chun-Chia Hsu

A THESIS

submitted to

Oregon State University

in partial fulfillment of

the requirements for the

degree of

Master of Science

Completed by December 3, 1991

Commencement June 1992

APPROVED:

Redacted for Privacy

Associate Professor of Mechanical Engineering
in charge of major

Redacted for Privacy

Head of Department of Mechanical Engineering

Redacted for Privacy

Dean of Graduate School

Date thesis is presented December 3, 1991

Typed by Chun-Chia Hsu for Chun-Chia Hsu

ACKNOWLEDGEMENTS

I would like to express my appreciation first to my major professor, Dr. Eugene Fichter, and his wife Dr. Becky L. Fichter. They have spent much time in consultation and provided valuable suggestions during this research. Without their help and encouragement, this thesis could not have been finished.

I would like to thank all my friends, especially Mr. Foo and Miss Cho, for their suggestions, encouragement and care.

I also want to thank all the teachers who have taught me before. I can not have this time without their teaching and guidance.

Finally, particular acknowledgement goes to my parents. Their endless financial, non-technical support and encouragement, let me complete this degree.

TABLE OF CONTENTS

LIST OF FIGURES

LIST OF TABLES

LIST OF APPENDIX TABLES

RANGE OF MOTION OF BEETLE BODY AS A FUNCTION OF LEG PARAMETERS

1. INTRODUCTION

1.1. Why study beetle's body range of motion with different link parameters?

In recent years walking machines have been the subject of considerable study because, in complicated environments, walking machines, or legged vehicles, have advantages over tracked or wheeled vehicles. Approximately 50% of land surface of earth is not accessible to conventional tracked or wheeled vehicles (Song and Waldron 1989). Walking machines can travel over irregular terrains, across areas of soft soil, on steep inclines or in open-work structures. They can do this while using less fuel and causing less environmental damage than tracked or wheeled vehicles (Song and Waldron 1989). Moreover, the legs of walking machines can be used as secondary arms for either digging or gripping (Todd 1985).

The body range of motion is the set of all possible positions and orientations of the beetle body with feet in fixed positions. This set constitutes the reachable workspace of the body of with that set of fixed foot

positions. This information is valuable for analyzing walking of beetles and for design of walking machines. For the current study, body range of motion is defined as the ranges of motion of body mass center.

In this study, the underlying research question is the issue of what effects is served by changes to the leg parameters of the darkling beetle. Some specific leg parameters are selected for changing. Body ranges of motion are searched based on these changes. From these body's ranges, we can understand which limitations or changes are appropriate for effective design and manufacture of walking machine.

1.2. Modeling of the darkling beetle

In recent years, walking machines have been designed for proof-of-concept of control and navigation system while travelling on obstacle-free surfaces which are nearly horizontal and smooth in nature (Baek 1990). Walking machines currently in use do not perform well in complex environments since their leg mechanisms and controls have not been designed to accommodate difficult terrains. Thus, the ability of animals which can travel over varying and difficult terrain has been a source of inspiration for research into walking machine design.

Among animal life, arthropods and vertebrates are

the only candidates for biological research in legged locomotion (Pedley 1977, Gewecke and Wendler 1985) for reason of their multi-segmented articulated legs. Arthropods have evolved to deal with a wide variety of terrain (i.e., spatially complex environment) over a period of 600 million years (Fichter et al. 1987). Vertebrates have sophisticated nervous systems and internal skeletons. Arthropods, including lobsters, spiders, crabs and insects, possess simple nervous systems and external skeletons. Simple nervous systems imply relatively simple control systems which may be simulated in walking machines. External skeletons make it easy to identify joints axes of legs and observe their motions. So, the arthropods is a better selection for a model of walking machine.

If an animal's locomotion is confined to walking or running on the ground, it will be able to provide a good model of walking machine. The darkling beetle, ***Eleodes obscura sulcipennis***, has been chosen since it neither flies nor jumps and is easily available. Darkling beetles are common in arid regions of the western USA. In addition, the darkling beetles is easily handled for reason of its relatively large size about 30 mm, from head to tail, and durable body.

1.3. Subjects discussed in this thesis

Chapter 2, defines coordinate systems for the body and legs of the darkling beetle using the D-H (Denavit-Hartenberg) model (Denavit and Hartenberg, 1955).

Chapter 3 presents the derivation of kinematic equations for legs and the solution of these equations. The quartic equation resulting from this solution is solved in chapter 4 using Bairstow's method. Finally, all inverse kinematic solutions are obtained for each leg and use to determine acceptable points within the range of motion.

For tracing the boundary of the body range of motion, an algorithm developed by Mason (1956), Cordray (1957) and Mason (1957) is presented in chapter 5. This chapter discusses the search method for closed loop contours, the set of initial conditions for starting boundary searching and giving examples of "sub-space" and "split-workspace" (Foo 1991). It also explains the computer programs developed for use in this study.

Chapter 6 discusses how to find foot positions of six legs for best body ranges of motion. At the beginning of this chapter link parameters changes are discussed.

Discussions of foot and body ranges of motion with changed link parameters and feet fixed on the ground are

presented in chapter 7. The effects of roll, pitch, yaw and numerical method are considered in the end of this chapter.

2. DEFINITION OF COORDINATE SYSTEMS FOR THE BEETLE

Setting coordinate systems for darkling beetle is the first and most important step, otherwise the kinematic equations for beetle's legs can not be written. There are five segments, coxa, trochanter, femur, tibia and tarsus, in each leg of the darkling beetle, as shown in Fig. 2.1. The first four are connected by revolute joints and a ball-and-socket joint is used to join tibia and tarsus together. Since all subsegments of tarsus touch ground during walking and tarsus is not related to the leg movement of beetle, this segment has been eliminated from consideration of leg composition. The trochanter is assumed fused to femur because its motion relative to the femur is small. So, for the purpose of this study, the coxa-trochanter joint is included in coxa-femur joint. Based upon these assumptions, the leg is joined by three revolute joints which can be modeled as a RRR manipulator.

For determining measurement of link parameters of beetle, a measuring coordinate system (^{M}x, ^{M}y, ^{M}z) is defined. The origin of this coordinate system is located at the midpoint of the line segment connecting ventral articulations of middle legs (Figs. 2.1 and 2.2). The axis ^{M}x lies along this line segment, positive toward beetle's right side. The axis ^{M}y intersects the line

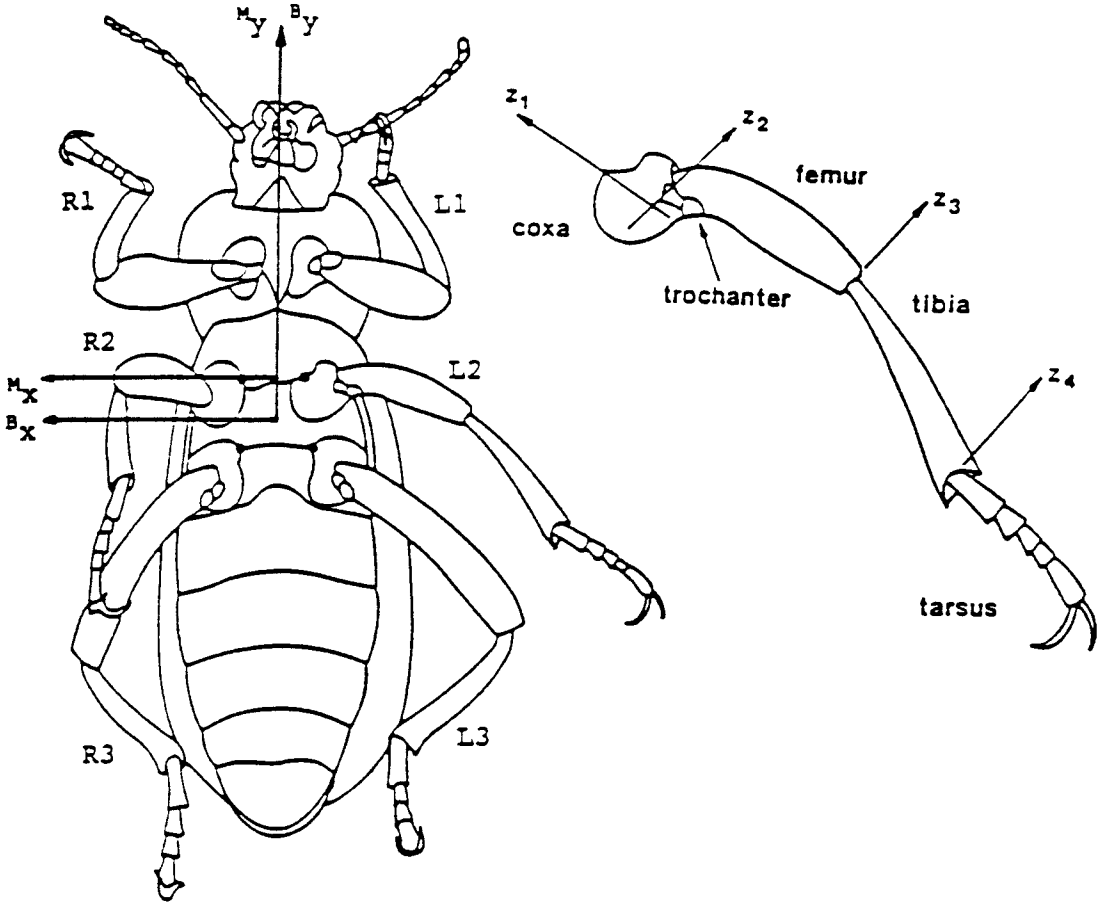

Fig. 2.1. Ventral view of a darkling beetle showing segment names, body and measuring coordinate systems and joint axes of left middle leg (Baek 1990).

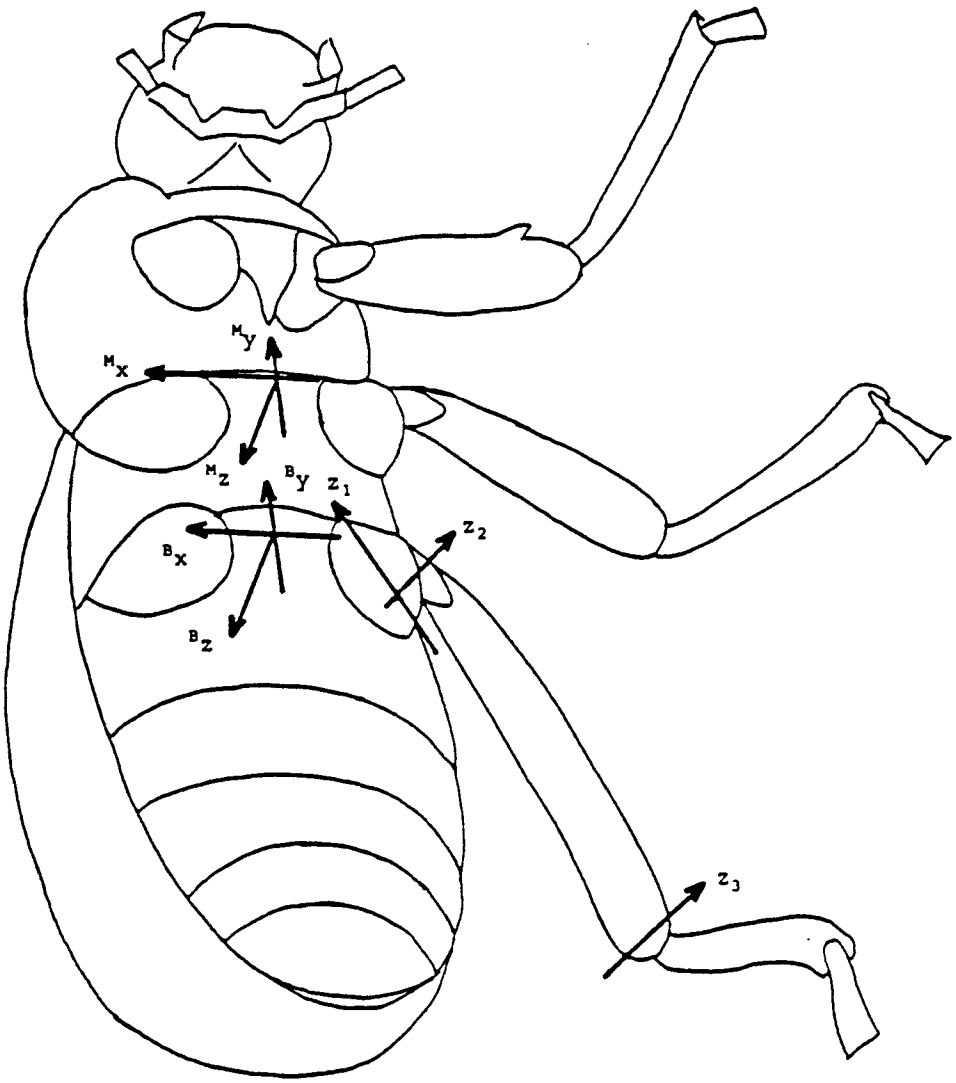

Fig. 2.2. Perspective view of a darkling beetle showing joint axes of left hind leg, measuring and body coordinate systems (Baek 1990).

connecting ventral articulations of rear legs, positive toward head. The axis ^{M}z forms a right-handed coordinate system (Fig. 2.2). Fig. 2.1 also shows the leg numbering system. According to the beetle's external skeletons and the shape of body, including legs, two assumptions are used to simplify this kinematic study.

1) The body is rigid,

2) The body has mirror symmetry about the ^{M}y-^{M}z plane.

The first is justified because the beetle has an external skeleton; structurally this is a shell making it very rigid for its weight. The second assumption is

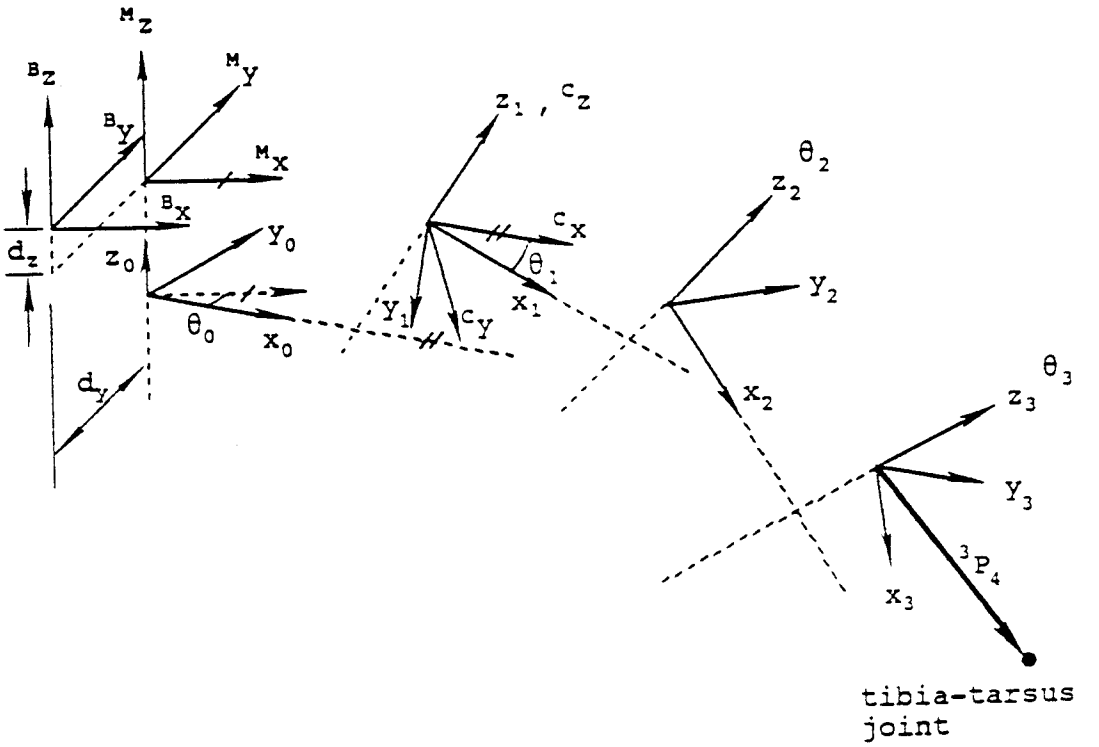

Fig. 2.3. Coordinate systems of leg of beetle in D-H notation (Baek 1990).

certainly an approximation but one which is generally made about these animals and accurate as an average over many individuals.

Fig 2.3 shows body coordinate system (${}^{B}x$, ${}^{B}y$, ${}^{B}z$), coordinate systems for simplifying model (frames "0" and "c") and coordinate system for leg segments. Axes of the body coordinate system (${}^{B}x$, ${}^{B}y$, ${}^{B}z$) are parallel to the measuring coordinate system (${}^{M}x$, ${}^{M}y$, ${}^{M}z$) respectively and the origin of body coordinate system is placed at body's center of mass. The coordinate system "0" (x_0, y_0, z_0) is used between body-coxa coordinate system and measuring coordinate system to apply Denavit-Hartenberg notation (D-H notation). The frame "c" (${}^{c}x$, ${}^{c}y$, ${}^{c}z$) is placed between the frames "0" and "1" to simplify derivation of inverse kinematic equations. The kinematic parameters for all legs were measured on dead beetles using the procedures described in Fichter et al (1988). The kinematic parameters for six legs are listed from tables 2.1 to 2.6.

Table 2.1. Kinematic parameters for right front leg

Segment	Link length (mm)	Link twist (deg)	Link offset (mm)	Range of joint angle (deg)
Body	3.38	-141.0	-1.32	101.7 to 101.7
Coxa	0.24	-100.4	-2.81	4.2 to 114.2
Femur	3.02	27.9	16.24	-89.8 to 20.2
Tibia	6.93	0.0	-13.19	-110.4 to 29.6

Table 2.2. Kinematic parameters for right middle leg

Segment	Link length (mm)	Link twist (deg)	Link offset (mm)	Range of joint angle (deg)
Body	0.21	-147.6	-2.27	81.5 to 81.5
Coxa	1.34	100.7	-3.47	46.8 to 161.8
Femur	4.58	-11.3	37.35	-24.8 to 85.2
Tibia	7.48	0.0	-35.29	-26.6 to 113.4

Table 2.3. Kinematic parameters for right hind leg

Segment	Link length (mm)	Link twist (deg)	Link offset (mm)	Range of joint angle (deg)
Body	1.98	136.4	-3.24	-120.7 to -120.7
Coxa	0.94	98.6	-5.57	-108.2 to -43.2
Femur	11.28	-12.6	4.93	-110.5 to 24.5
Tibia	10.35	0.0	-1.34	26.2 to 166.2

Table 2.4. Kinematic parameters for left front leg

Segment	Link length (mm)	Link twist (deg)	Link offset (mm)	Range of joint angle (deg)
Body	3.38	141.0	-1.32	78.3 to 78.3
Coxa	0.24	100.4	-2.81	-114.2 to -4.2
Femur	3.02	-27.9	16.24	-20.2 to 89.8
Tibia	6.93	0.0	-13.19	-29.6 to 110.4

Table 2.5. Kinematic parameters for left middle leg

Segment	Link length (mm)	Link twist (deg)	Link offset (mm)	Range of joint angle (deg)
Body	0.21	147.6	-2.27	98.5 to 98.5
Coxa	1.34	-100.7	-3.47	-161.8 to -46.8
Femur	4.58	11.3	37.35	-85.2 to 24.8
Tibia	7.48	0.0	-35.29	-113.4 to 26.6

Table 2.6. Kinematic parameters for left hind leg

Segment	Link length (mm)	Link twist (deg)	Link offset (mm)	Range of joint angle (deg)
Body	1.98	-136.4	-3.24	-59.3 to -59.3
Coxa	0.94	-98.6	-5.57	43.2 to 108.2
Femur	11.28	12.6	4.93	-24.5 to 110.5
Tibia	10.35	0.0	-1.34	-166.2 to -26.2

3. DERIVATION AND SOLUTION OF KINEMATIC EQUATION

Kinematic equations are used to compute position of the end-effector relative to the base of the manipulator as a function of the joint variables (Craig 1986). In this thesis the inverse kinematic equations are used to calculate joint variables from the position of the end-effector. Because all six legs of beetle are RRR manipulator, only one set of inverse kinematic equations is needed. The link parameters of each leg are substituted into the inverse kinematic equations to solve for joint variables. Therefore, for a given body position and a known set of foot positions, all joint variables can be solved for. If all joint variables are within their ranges then this body position can be said to be within the body's range motion for the known set of foot position.

The global coordinate system (${}^{G}x$, ${}^{G}y$, ${}^{G}z$) can be put at any point and positive ${}^{G}z$ axis is opposite gravity force direction. Relationship between body and global coordinate systems can be shown by a homogeneous transformation matrix. The transformation from global to body coordinate system can be

${}^{G}T_{B}=\text{Trans}(x_B, y_B, z_B)\ \text{Rot}({}^{G}y, \phi_2)\ \text{Rot}({}^{G}x, \phi_1)\ \text{Rot}({}^{G}z, \phi_3)$

where ϕ_1, ϕ_2 and ϕ_3 are orientation angles of the body about ${}^{G}x$, ${}^{G}y$ and ${}^{G}z$ axes and these three angles are

conventionally called pitch, roll and yaw respectively.

Let ${}^{M}\mathbf{d}_B$ be the position vector of center-of-mass of body with respect to measuring coordinate system. So, ${}^{M}\mathbf{d}_B = d_x\ {}^{M}\mathbf{n}_x + d_y\ {}^{M}\mathbf{n}_y + d_z\ {}^{M}\mathbf{n}_z$ where ${}^{M}\mathbf{n}$'s are the unit vectors of the measuring coordinate system and d_x is zero (because of beetle's body symmetry). Then, the transformation matrix from body to measuring coordinate system is

$$ {}^{M}T_B = \begin{bmatrix} 1 & 0 & 0 & d_x \\ 0 & 1 & 0 & d_y \\ 0 & 0 & 1 & d_z \\ 0 & 0 & 0 & 1 \end{bmatrix} $$

where

$$ d_x = 0 $$

The general formula of the homogeneous transformation matrix for each link using the D-H parameters (Craig 1986) is

$$ {}^{i-1}T_i = \begin{bmatrix} C\theta_i & -S\theta_i & 0 & a_{i-1} \\ S\theta_i C\alpha_{i-1} & C\theta_i C\alpha_{i-1} & -S\alpha_{i-1} & -S\alpha_{i-1} d_i \\ S\theta_i S\alpha_{i-1} & C\theta_i S\alpha_{i-1} & C\alpha_{i-1} & C\alpha_{i-1} d_i \\ 0 & 0 & 0 & 1 \end{bmatrix} $$

where

$i = 0, 1, 2, 3$

$C\theta_i = \cos \theta_i$

$S\theta_i = \sin \theta_i$

$C\alpha_i = \cos \alpha_i$

$S\alpha_i = \sin \alpha_i$

a_i= the distance from z_i to z_{i+1} measured along x_i.

α_i= the angle between z_i and z_{i+1} measured about x_i.

d_i= the distance from x_{i-1} to x_i measured along z_i.

θ_i= the angle between x_{i-1} and x_i measured about z_i.

If i-1 is -1, it means frame "-1" is equivalent to the measuring coordinate system "M". From Fig. 2.3, θ_0 is a constant value. Hence, θ_1, θ_2 and θ_3 are the only unknown variables.

Coordinate of the central point of the tibia-tarsus joint can be formed by two paths. One is to define ${}^{G}P_4$ from the global coordinate system. The other is expressed in the left hand side of the following equation.

$$ {}^{G}T_B \; {}^{B}T_M \; {}^{M}T_0 \; {}^{0}T_1 \; {}^{1}T_2 \; {}^{2}T_3 \; {}^{3}P_4 = {}^{G}P_4 \qquad (3.1) $$

Equation (3.1) can be simplified by separating the variable θ_1 from constant values, a_0, α_0 and d_1, in the matrix ${}^{0}T_1$ and introducing frame "c" between frames "0" and "1" (Fig. 2.3). So, a new definition equation will be given as ${}^{0}T_1 = {}^{0}T_c \; {}^{c}T_1$ where

$${}^{c}T_1 = \mathrm{Rot}(z_1, \theta_1)$$

and

$$ {}^{0}T_{c} = \mathrm{Rot}(x, \alpha_0)\ \mathrm{Trans}(x, a_0)\ \mathrm{Trans}(z, d_1) $$

Therefore,

$$ {}^{c}T_1\ {}^{1}T_2\ {}^{2}T_3\ {}^{3}P_4 = {}^{c}P_4 \qquad (3.2) $$

and

$$ {}^{c}P_4 = {}^{c}T_0\ {}^{0}T_M\ {}^{M}T_B\ {}^{B}T_G\ {}^{G}P_4 \qquad (3.3) $$

These equations are the kinematic equations of one leg. The right-hand side of equation (3.3) and the left-hand side of equation (3.2) are known. Thus, all knowns are substituted into equations (3.2) and (3.3). After expanding and calculating, equation (3.2) becomes to three nonlinear scalar equations (equations 3.4 to 3.6) with three unknown variables, θ_1, θ_2 and θ_3 (Baek 1990) and ${}^{c}P_4({}^{c}P_{4x}, {}^{c}P_{4y}, {}^{c}P_{4z})$ is obtained from equation (3.3), too.

$$ {}^{c}P_{4x} = E_1\ C\theta_1 + E_2\ S\theta_1 \qquad (3.4) $$

$$ {}^{c}P_{4y} = -E_2\ C\theta_1 + E_1\ S\theta_1 \qquad (3.5) $$

and

$$ R_1 = Q_{11}\ S\theta_3 + Q_{12}\ C\theta_3 \qquad (3.6) $$

where

$$ E_1 = (C\theta_2\ C\theta_3 - S\theta_2\ S\theta_3\ C\alpha_2)\ {}^{3}P_{4x} + (-C\theta_2\ S\theta_3 - S\theta_2\ C\theta_3\ C\alpha_2)\ {}^{3}P_{4y} + S\theta_2\ S\alpha_2\ {}^{3}P_{4z} + C\theta_2\ a_2 + S\theta_2\ S\alpha_2\ d_3 + a_1 $$

$$ E_2 = (-S\theta_2\ C\theta_3\ C\alpha_1 - C\theta_2\ S\theta_3\ C\alpha_1\ C\alpha_2 + S\theta_3\ S\alpha_1\ S\alpha_2)\ {}^{3}P_{4X} + (S\theta_2\ S\theta_3\ C\alpha_1 - C\theta_2\ C\theta_3\ C\alpha_1\ C\alpha_2 + C\theta_3\ S\alpha_1\ S\alpha_2)\ {}^{3}P_{4y} + (C\theta_2\ C\alpha_1\ S\alpha_2 + S\alpha_1\ C\alpha_2)\ {}^{3}P_{4z} + (-S\theta_2\ C\alpha_1\ a_2 + C\theta_2\ C\alpha_1\ S\alpha_2\ d_3 + S\alpha_1\ d_2) $$

$$R_1 = {}^{c}P_{4z} - (-C\theta_2\ S\alpha_1\ S\alpha_2 + C\alpha_1\ C\alpha_2)\ {}^{3}P_{4z} - (S\theta_2\ S\alpha_1\ a_2 - C\theta_2\ S\alpha_1\ S\alpha_2\ d_3 + C\alpha_1\ C\alpha_2\ d_3 + C\alpha_1\ d_2)$$

$$Q_{11} = C\theta_2\ S\alpha_1\ C\alpha_2\ {}^{3}P_{4x} + C\alpha_1\ S\alpha_2\ {}^{3}P_{4x} - S\theta_2\ S\alpha_1\ {}^{3}P_{4y}$$

$$Q_{12} = S\theta_2\ S\alpha_1\ {}^{3}P_{4x} + C\theta_2\ S\alpha_1\ C\alpha_2\ {}^{3}P_{4y} + C\alpha_1\ S\alpha_2\ {}^{3}P_{4y}$$

Equations (3.4) and (3.5) are a circle and equation (3.6) is a quartic curve independent of θ_1 (Baek 1990). These three equations are all squared individually and then all three squared equations are summed together to form a new equation. After simplifying this new equation, equation (3.7) is gotten.

$$R_2 = Q_{21}\ S\theta_3 + Q_{22}\ C\theta_3 \qquad (3.7)$$

where

$$R_2 = {}^{c}P_{4X}{}^{2} + {}^{c}P_{4y}{}^{2} + {}^{c}P_{4z}{}^{2} - {}^{3}P_{4x}{}^{2} - {}^{3}P_{4y}{}^{2} - {}^{3}P_{4z}{}^{2} - a_1{}^{2} - a_2{}^{2} - d_2{}^{2} - d_3{}^{2} - 2\ (C\theta_2\ a_1\ a_2 + C\alpha_2\ d_2\ d_3 + S\theta_2\ S\alpha_2\ a_1\ d_3 + d_3\ {}^{3}P_{4z} + C\alpha_2\ d_2\ {}^{3}P_{4z} + a_1\ S\theta_2\ S\alpha_2\ {}^{3}P_{4z})$$

$$Q_{21} = 2\ (S\alpha_2\ d_2\ {}^{3}P_{4x} - a_1\ S\theta_2\ C\alpha_2\ {}^{3}P_{4x} - a_2\ {}^{3}P_{4y} - C\theta_2\ a_1\ {}^{3}P_{4y})$$

$$Q_{22} = 2\ (a_2\ {}^{3}P_{4x} + C\theta_2\ a_1\ {}^{3}P_{4x} + d_2\ S\alpha_2\ {}^{3}P_{4y} - S\theta_2\ C\alpha_2\ a_1\ {}^{3}P_{4y})$$

From equations (3.6) and (3.7), $S\theta_3$ and $c\theta_3$ can be solved. Therefore,

$$S\theta_3 = \Omega_1 / \Delta \qquad (3.8)$$

$$c\theta_3 = \Omega_2 / \Delta \qquad (3.9)$$

where

$$\Delta = Q_{11}\ Q_{22} - Q_{12}\ Q_{21}$$

$$\Omega_1 = Q_{22}\ R_1 - Q_{12}\ R_2$$

$$\Omega_2 = Q_{11}\ R_2 - Q_{21}\ R_1$$

Since $\cos^2\theta + \sin^2\theta = 1$, the above equations can be eliminated θ_3 and simplified as a new equation which only is a function of θ_2.

Therefore,

$$\Delta^2 = \Omega_1^2 + \Omega_2^2 \qquad (3.10)$$

where

$$\Delta = H_1\ C\theta_2 + H_2\ S\theta_2 + H_3$$

$$\Omega_1 = I_1\ S\theta_2 + I_2\ C\theta_2 + I_3$$

$$\Omega_2 = J_1\ S\theta_2 + J_2\ C\theta_2 + J_3$$

and

$$H_1 = 2\ (S\alpha_1\ C\alpha_2\ a_2 + a_1\ C\alpha_1\ S\alpha_2)\ ({}^3P_{4x}{}^2 + {}^3P_{4y}{}^2)$$

$$H_2 = -2\ S\alpha_1\ S\alpha_2\ d_2\ ({}^3P_{4x}{}^2 + {}^3P_{4y}{}^2)$$

$$H_3 = 2\ (a_1\ S\alpha_1\ C\alpha_2 + C\alpha_1\ S\alpha_2\ a_2)\ ({}^3P_{4x}{}^2 + {}^3P_{4y}{}^2)$$

$$I_1 = G_9\ D_6 - G_7\ D_4 - G_4\ D_8 - G_5\ D_9$$

$$I_2 = G_4\ D_7 + G_6\ D_9 + G_8\ D_6 - G_7\ D_5$$

$$I_3 = G_5\ D_8 + G_9\ D_4 + G_4\ D_9 - G_7\ D_6$$

$$J_1 = G_1\ D_8 + G_2\ D_9 - G_7\ D_2 - G_9\ D_3$$

$$J_2 = G_7\ D_1 - G_8\ D_3 - G_1\ D_7 - G_3\ D_9$$

$$J_3 = G_9\ D_2 - G_2\ D_8 + G_7\ D_3 - G_1\ D_9$$

and in addition,

$$D_1 = S\alpha_1\ C\alpha_2\ {}^3P_{4x}$$

$$D_2 = S\alpha_1\ {}^3P_{4y}$$

$$D_3 = C\alpha_1\ S\alpha_2\ {}^3P_{4x}$$

$$D_4 = S\alpha_1\ C\alpha_2\ {}^3P_{4x}$$

$D_5 = S\alpha_1\ C\alpha_2\ {}^3P_{4y}$

$D_6 = C\alpha_1\ S\alpha_2\ {}^3P_{4y}$

$D_7 = (d_3 + {}^3P_{4z})\ S\alpha_1\ S\alpha_2$

$D_8 = a_2\ S\alpha_1$

$D_9 = {}^cP_{4z} - C\alpha_1\ d_2 - C\alpha_1\ C\alpha_2\ d_3 - C\alpha_1\ C\alpha_2\ {}^3P_{4z}$

$G_1 = 2\ (S\alpha_2\ d_2\ {}^3P_{4x} - a_2\ {}^3P_{4y})$

$G_2 = 2\ a_1\ C\alpha_2\ {}^3P_{4x}$

$G_3 = 2\ a_1\ {}^3P_{4y}$

$G_4 = 2\ (a_2\ {}^3P_{4x} + d_2\ S\alpha_2\ {}^3P_{4y})$

$G_5 = 2\ C\alpha_2\ a_1\ {}^3P_{4y}$

$G_6 = 2\ a_1\ {}^3P_{4x}$

$G_7 = {}^cP_{4x}{}^2 + {}^cP_{4y}{}^2 + {}^cP_{4z}{}^2 - {}^3P_{4x}{}^2 - {}^3P_{4y}{}^2 - {}^3P_{4z}{}^2 - a_1{}^2 - a_2{}^2 - d_2{}^2 - d_3{}^2 - 2\ (C\alpha_2\ d_2\ d_3 + d_3\ {}^3P_{4z} + C\alpha_2\ d_2\ {}^3P_{4z})$

$G_8 = 2\ a_1\ a_2$

$G_9 = 2\ (S\alpha_2\ a_1\ d_3 + a_1\ S\alpha_2\ {}^3P_{4z})$

Rearrange the equation (3.10) with respect to θ_2 and simplify, results in:

$$K_1 S\theta_2{}^2 + K_2 C\theta_2{}^2 + K_3 C\theta_2 S\theta_2 + K_4 S\theta_2 + K_5 C\theta_2 + K_6 = 0 \qquad (3.11)$$

where

$K_1 = I_1{}^2 + J_1{}^2 - H_2{}^2$

$K_2 = I_2{}^2 + J_2{}^2 - H_1{}^2$

$K_3 = 2\ (I_1\ I_2 + J_1\ J_2 - H_1\ H_2)$

$K_4 = 2\ (I_1\ I_3 + J_1\ J_3 - H_2\ H_3)$

$K_5 = 2\ (I_2\ I_3 + J_2\ J_3 - H_1\ H_3)$

$K_6 = I_3{}^2 + J_3{}^2 - H_3{}^2$

Since $\sin^2\theta_2 + \cos^2\theta_2 = 1$, $\sin\theta_2$ can be eliminated from equation (3.11) giving:

$$K_7 X^4 + K_8 X^3 + K_9 X^2 + K_{10} X + K_{11} = 0 \qquad (3.12)$$

where

$$K_7 = (K_2 - K_1)^2 + K_3^2$$

$$K_8 = 2 [K_5 (K_2 - K_1) + K_3 K_4]$$

$$K_9 = K_5^2 + K_4^2 - K_3^2 + 2 (K_2 - K_1)(K_1 + K_6)$$

$$K_{10} = 2 [K_5 (K_1 + K_6) - K_3 K_4]$$

$$K_{11} = (K_1 + K_6)^2 - K_4^2$$

and

$$X = \cos\theta_2$$

Equation (3.12), a quartic equation, can be solved by Bairstow method, a numerical method, used to calculate roots of polynomial equations. This method is given detailed consideration in chapter 4.

Equation (3.12) may have 4, 2 or no real roots; if there are no real roots the body position is outside the range of motion.

From equation (3.11),

$$\sin\theta_2 = \frac{\cos^2\theta_2(K_1 - k_2) - (k_5\cos\theta_2 + K_6 + K_1)}{K_3\cos\theta_2 + K_4}$$

Real roots are substituted into above equation to calculate values of $\sin\theta_2$. The $\sin\theta_2$ can be solved

from $\sin^2\theta_2 = 1 - \cos^2\theta_2$, too. Since sin θ_2 is equal to $(1-\cos^2\theta_2)^{1/2}$ or $-(1-\cos^2\theta_2)^{1/2}$, the right solution does not obviously be confirmed from these two. Thus, this formula does not use in here. So θ_2 will be obtained by θ_2 = Atan2 (sin θ_2, cos θ_2) and θ_3 can be calculated from equations (3.8) and (3.9). In equations (3.4) and (3.5), E_1 and E_2 can be calculated and finally θ_1 can be determined.

Several sets of θ_1, θ_2 and θ_3 are found from above procedures for each of the six legs. If any of these sets satisfy the criteria:

$$(\theta_1)_{min} \leq \theta_1 \leq (\theta_1)_{max}$$

$$(\theta_2)_{min} \leq \theta_2 \leq (\theta_2)_{max}$$

and

$$(\theta_3)_{min} \leq \theta_3 \leq (\theta_3)_{max}$$

then the body position is within its range of motion.

4. NUMERICAL METHOD FOR SOLUTION OF QUARTIC EQUATION

4.1. Introduction

Either algebraic or numerical methods can be used to solve real-coefficient quartic equations. However, the numerical methods are much simpler and much less convoluted than the algebraic method; thus a numerical method is used. From many available numerical methods for solving polynomial equations, the Bairstow method was chosen for this study. The method seeks quadratic factors of a polynomial equation with real coefficients. The advantage of this method is that both imaginary and real roots can be easily found by solving the quadratic factors (Press, W.H., Flannery, B.P., Teukolsky, S.A. and Vetterling, W.T. 1989, Haberman 1966).

4.2. The Bairstow method

The Bairstow method divides the polynomial to be solved by a quadratic polynomial with real coefficients. Let

$$f(x)=a_0x^n+a_1x^{n-1}+\cdots\cdots+a_{n-1}x+a_n \qquad (4.1)$$

be a polynomial equation with real coefficients of degree n which will be divided by x^2+px+q where p and q are real numbers.

$$f(x)=(x^2+px+q)\,(b_0x^{n-2}+b_1x^{n-3}+\cdots\cdots+b_{n-2})+Rx+S$$

Expanding above equation f(x) becomes

$$f(x) = b_0x^n+(b_1+pb_0)\,x^{n-1}+(b_2+pb_1+qb_0)\,x^{n-2}+\cdots\cdots+$$
$$(R+pb_{n-2}+qb_{n-3})\,x+qb_{n-2}+S \qquad (4.2)$$

where R and S are the functions of p and q. If x^2+px+q is a factor of f(x), both R and S must be zero. Therefore,

$$R(p,q)=0$$
$$S(p,q)=0 \qquad (4.3)$$

Let p_0 and q_0 be assumed as approximate values of p and q. So,

$$p=p_0+\Delta p$$
$$q=q_0+\Delta q$$

and

$$R(p_0+\Delta p,\ q_0+\Delta q)=0$$
$$S(p_0+\Delta p,\ q_0+\Delta q)=0 \qquad (4.4)$$

The corrections, Δp and Δq, are calculated and added to previously assumed coefficients p_0 and q_0 to get a new pair of p and q for using in the next iteration. When Δp and Δq approach zero, the procedure converges to the required values of p and q. Thus the original polynomial is replaced by a quadratic and a new polynomial with degree two less than the original. Fig. 4.1 illustrates the flow chart for Bairstow method.

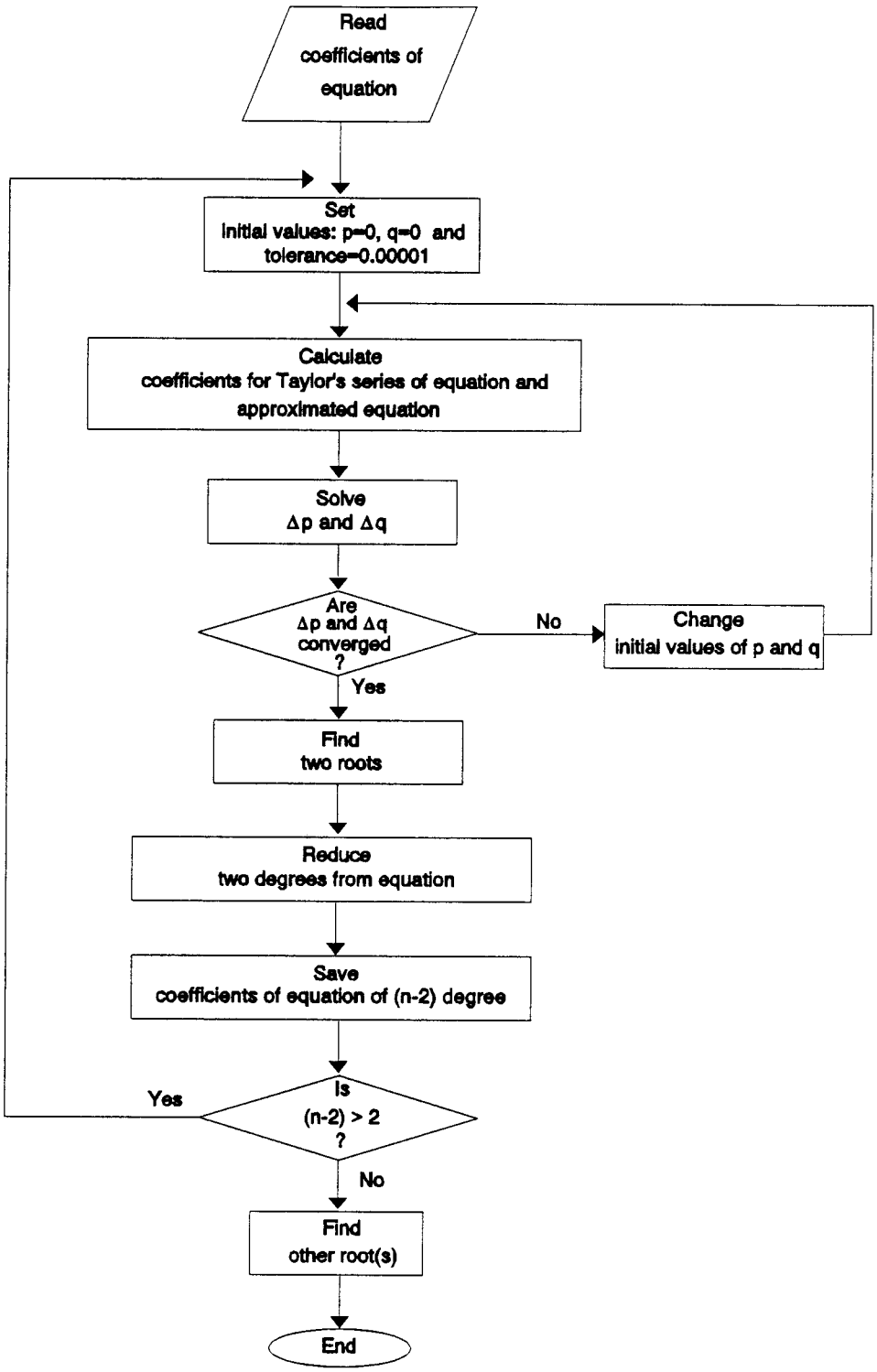

Fig. 4.1. Flow chart for the Bairstow method.

4.3. Derivation of two corrections: Δp and Δq

Equations (4.4) can be expanded in Taylor series as follows:

$$R(p_0+\Delta p, q_0+\Delta q) = R(p_0, q_0) + \Delta p \frac{\partial R}{\partial p} + \Delta q \frac{\partial R}{\partial q} + \cdots\cdots = 0$$

$$S(p_0+\Delta p, q_0+\Delta q) = S(p_0, q_0) + \Delta p \frac{\partial S}{\partial p} + \Delta q \frac{\partial S}{\partial q} + \cdots\cdots = 0$$

If Δp and Δq are small, the above both equations can be approximated by

$$R(p_0, q_0) + \Delta p \frac{\partial R}{\partial p} + \Delta q \frac{\partial R}{\partial q} = 0 \qquad (4.5)$$

$$S(p_0, q_0) + \Delta p \frac{\partial S}{\partial p} + \Delta q \frac{\partial S}{\partial q} = 0 \qquad (4.6)$$

To solve equations (4.5) and (4.6), coefficients of equation (4.1) and equation (4.2) are compared. The relationships are:

$b_0 = a_0$

$b_1 = a_1 - pb_0$

$b_2 = a_2 - pb_1 - qb_0$

.....

$\cdots\cdots\cdots$

$R = b_{n-1} = a_{n-1} - pb_{n-2} - qb_{n-3}$

$S = b_n + pb_{n-1} = a_n - qb_{n-2}$

In general,

$b_{-1} = b_{-2} = 0$

$b_k = a_k - pb_{k-1} - qb_{k-2}$

where

$k=0,1,2,3,4,\cdots\cdots, n-1$

Using these relationships partial derivatives, $\partial R/\partial p$, $\partial R/\partial q$, $\partial S/\partial p$ and $\partial S/\partial q$, are calculated and denoted by C's (Herriot 1963):

$$\frac{\partial b_k}{\partial p} = -C_{k-1}$$

$$\frac{\partial b_k}{\partial q} = -C_{k-2} \qquad (4.7)$$

where

$C_k = b_k - Pc_{k-1} - qC_{k-2} \qquad (k=0,1,2,3,\cdots\cdots,n)$

$C_{-1} = C_{-2} = 0$

The k used in equations (4.7) is replaced by n-1 to obtain first two equations in equations (4.8) and is replaced by n to obtain others in equations (4.8).

$$\frac{\partial R}{\partial p} = \frac{\partial b_{n-1}}{\partial p} = -C_{n-2}$$

$$\frac{\partial R}{\partial q} = \frac{\partial b_{n-1}}{\partial q} = -C_{n-3}$$

$$\frac{\partial S}{\partial P} = \frac{\partial b_{n}}{\partial p} = -C_{n-1}$$

$$\frac{\partial S}{\partial q} = \frac{\partial b_{n}}{\partial q} = -C_{n-2} \qquad (4.8)$$

To solve for Δp and Δq, equations (4.8) are substituted into simultaneous equations which are formed by equations (4.5) and (4.6). First, equation (4.5) is multiplied by p and subtracted from equation (4.6) to form a new equation. Since the R and S are known in equations (4.5) and (4.6), only the partial derivatives terms in this new equation and equation (4.5) are substituted by the known equations (4.8). After rearrangement, the corrections, Δp and Δq, can be solved by

$$C_{n-2}\Delta p + C_{n-3}\Delta q = b_{n-1}$$

$$(C_{n-1} - b_{n-1})\Delta p + C_{n-2}\Delta q = b_{n}$$

Thus,

$$\Delta p = \frac{D_1}{D} \quad \text{and} \quad \Delta q = \frac{D_2}{D}$$

where

$$D = C_{n-2}C_{n-2} - C_{n-3}(C_{n-1} - b_{n-1})$$

$$D_1 = b_{n-1}C_{n-2} - b_nC_{n-3}$$

$$D_2 = b_nC_{n-2} - b_{n-1}(C_{n-1} - b_{n-1})$$

5. ALGORITHM FOR FINDING BOUNDARY OF BODY RANGE

5.1. Introduction

Body range of motion (workspace) with fixed foot positions is constituted of all positions of center of mass for which there are solutions for inverse kinematic equations for all legs. The boundary of this workspace is to be found. But there is no functional description of the boundary; only the ability to determine if a point is inside or outside. The first step will be to consider only the curves of intersection of the boundary with a set of equally spaced planes parallel to the global x-y plane.

To locate the boundary curves in these planes, an algorithm which was developed by Mason (1956), Cordray (1957) and Mason (1957) is used in this study. Fichter (1986) used this method before to obtain range of motion for a Stewart Platform. The algorithm of Mason and Cordray was developed to get contour maps in a 2-D plane which provided pictorial information about the orientation and spacing of atoms and molecules in a crystal. In this algorithm, the 2-D plane is divided by horizontal and vertical lines with the same intervals. The searching algorithm then finds meshpoints which lie approximately on the contour boundary.

5.2. Searching method for finding contour

The algorithm proceeds as follows. If one side of a unit square crosses the boundary, two points on this side will be on opposite sides of the boundary and will be numbered 1 and 4. The point 1 is assumed as within the boundary and the point 4 is assumed as outside the boundary. The other two corners of the unit square are numbered 2 and 3 (Fig. 5.1). From Fig. 5.1, the contour can enter the unit square from one of four directions: right, left, top and bottom.

If contour enters from either top or bottom, the x coordinates of points 1 and 2 are equal as are x coordinates of points 3 and 4 and y coordinates of points 2 and 3 are decreased or increased one unit distance from points 1 and 4. If contour enters from either left or

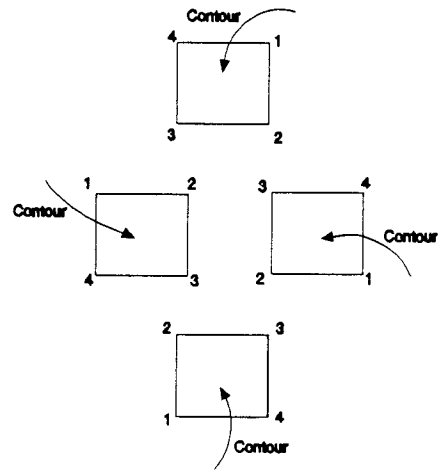

Fig. 5.1. Possibilities of contour entries and numbers for four corners of square grid.

right, then the y coordinates of points 1 and 2 are equal as are those of points 3 and 4 and x coordinates are increased or decreased one unit distance from points 1 and 4. Because the grid is a square unit distances in x and y directions will be the same. But how can the entering directions be known? The coordinates of points 1 (within the boundary) and 4 (outside the boundary) can tell this.

1) y coordinates of points 1 and 4 are same:
   i) If x coordinate of point 1 is greater than point 4, then the contour enters from top of square.
   ii) If x coordinate of point 1 is less than point 4, then the contour enters from bottom of square.
2) x coordinates of points 1 and 4 are same:
   i) If y coordinate of point 1 is greater than point 4 then the contour enters from left of square.
   ii) If y coordinate of point 1 is less than point 4 then the contour enters from right of square.

From above rules, the following equations can be applied to determine coordinates of points 2 and 3.

1) If $y_1 = y_4$ and $x_1 > x_4$,
   then $x_2 = x_1$, $x_3 = x_4$, $y_2 = y_1 - \Delta d$, $y_3 = y_4 - \Delta d$
2) If $y_1 = y_4$ and $x_1 < x_4$,
   then $x_2 = x_1$, $x_3 = x_4$, $y_2 = y_1 + \Delta d$, $y_3 = y_4 + \Delta d$
3) If $x_1 = x_4$ and $y_1 > y_4$,
   then $y_2 = y_1$, $y_3 = y_4$, $x_2 = x_1 + \Delta d$, $x_3 = x_4 + \Delta d$

4) If $x_1 = x_4$ and $y_1 < y_4$,

then $y_2 = y_1$, $y_3 = y_4$, $x_2 = x_1 - \Delta d$, $x_3 = x_4 - \Delta d$

where x_i and y_i are the coordinates of point i

$i = 1, 2, 3, 4$

Δd = the length of one side of square grid

To eliminate some unwanted points during calculation, a variable, S, is used. S can be either 1 or -1 depending on where the contour leaves the previous square. S is 1 if the contour left the previous square through side 3-4. S is -1 if the contour left the previous square through side 1-2. S remains unchanged if the contour left the previous square through side 2-3. After determining the value of S, either point 2 or 3 will be selected to compute based on the value of S. When the needed point (point 2 or 3) is determined, one side (side 1-2 or 3-4) of unit grid is checked whether the boundary crosses. If the boundary crosses either side, new S and points 1 and 4 can be decided for next iteration and boundary point is found by interpolating between points 1 and 4. Above procedures can eliminate one meshpoint's calculation. If boundary does not cross above selected sides, the other unselected point will be computed to determine which side is crossed by boundary. Thus, new S and points 1 and 4 can be decided and boundary point is found after these procedures. These procedures will be repeated until the initial point

(introduced in next section) is found again. A flow chart of this method is shown in Fig. 5.2.

5.3. Initial conditions for searching method

To start boundary search, an initial point must be determined. The centroid of the six foot positions in x-y plane is located. The boundary of range of motion intersects a line which passed through this centroid and is parallel to the y-axis. Therefore, the initial search for boundary is begun from the centroid of positions along this line to the minimum and maximum y-coordinate values. Since the length of beetle body, from head to tail, is about 30 mm the minimum y is centroid of foot positions minus 30 and the maximum y is centroid of foot positions plus 30. The first direction of initial search is from the centroid to the maximum y-coordinate. When a boundary point is detected, the contour is traced and points 1 and 4 of this first grid are kept to examine whether the search procedure is finished or not. After completion of the search, the direction is changed toward to minimum y-coordinate discarding the area of previous contour to find whether another contour exists.

A flag variable is used while determining whether or not the boundary crosses the line through the centroid. If the starting point is within the boundary, the flag is

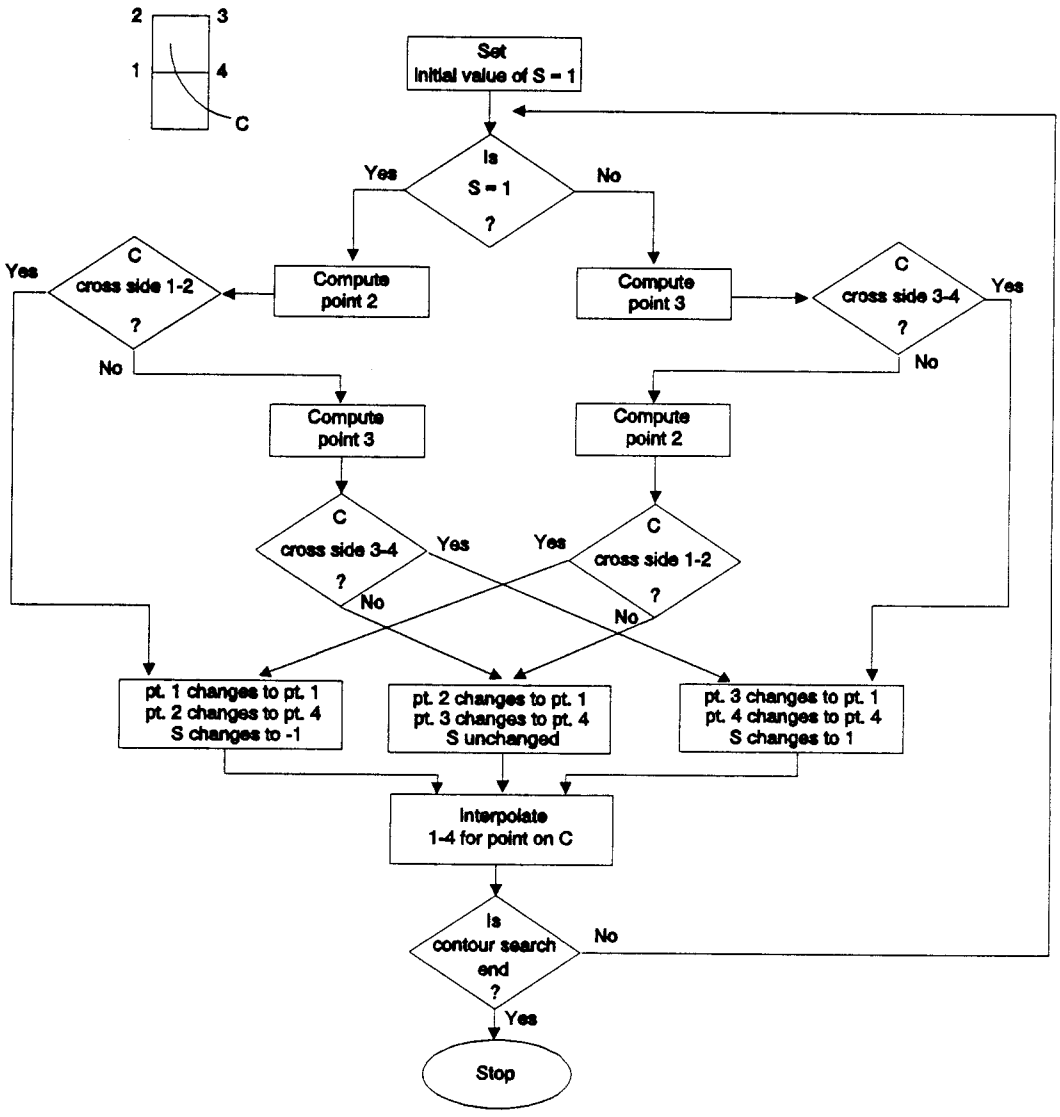

Fig. 5.2. Flow chart for Mason and Cordray algorithm.

1; otherwise, the flag is -1. When the flag changes from 1 to -1 or -1 to 1, the boundary has been crossed. Then,the search procedure is run until returning to points 1 and 4 of the first grid.

5.4. Computer program for searching range of motion

To search ranges of motion, a computer program was written in the C language. In this program, inputs and outputs are stored in files. The input files include leg parameters of the darkling beetle and foot positions, and the output files consist of the x-, y- and z-coordinates of the boundary points. The program also provides a graphic function which can display four views of the range of motion: front, top, side and axonometric projection views. The axonometric view can be rotated about y and z axes by user input of rotation angles.

The program has four principal subroutines which can be used independently. The Bairstow method for solving quartic equations was written first. The subroutine is limited to calculating the roots of quartic equations.

To determine the joint angles (θ_1, θ_2, θ_3) for a certain body point within boundary or not, the kinematic equations derived in chapter 3 were used to develop the second subroutine which also uses the first subroutine for solving quartic equations. The link parameters and

foot position files are the inputs for this program. The joint angles (θ_1, θ_2, θ_3) are found for six legs after calculating the inverse kinematic equations and these are compared with the ranges of each respective leg's joint angles to determine whether or not this certain point satisfied the beetle's limitations.

The third subroutine finds boundary points. In this subroutine, size of grid and number of iterations applied to interpolate the boundary points affect the accuracy of the results. A small number of iterations speeds computation but gives less accurate. A large size of grid can save time in running the program but can not give accurate curves especially for sharp corners (Fig.

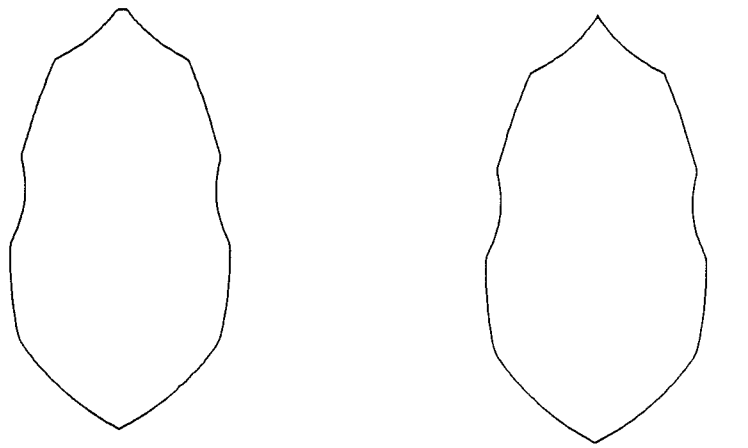

Fig. 5.3. Two different grid sizes for same contour.

5.3). For this study, the grid size 0.2 × 0.2 mm^2 is selected. During search procedure, each point is checked by solving for joint angles for each leg. If body range is to be determined, each point must be checked for inverse kinematic solutions of all six legs. If foot range is to be determined, only one leg's inverse kinematic solution is checked for each point. When a boundary point is found, its x-, y- and z-coordinates are saved in a data file.

The final subroutine is a graphic presentation of the contour on screen in top, front, side and axonometric views. It reads data from output file of search subroutine and shows all four views or only one.

5.5. Examples of special contours

Two kinds of special contours, split-workspace (Fig. 5.4) and sub-space (Fig. 5.5), (Foo, 1991) are considered in this study. As noted in the previous section, the search is begun from the centroid of six foot positions along the line passing through it. After one contour is found, the rest of this line is checked to determine if another boundary exists. If another contour is found split-workspace exists.

Within a contour of range of motion, a space which the beetle can not reach is called sub-space (Fig. 5.5).

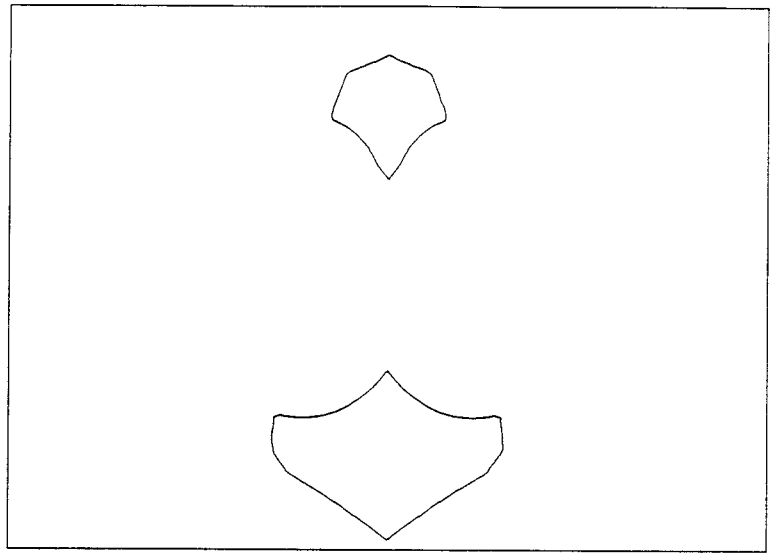

Fig. 5.4. An example of split-workspace.

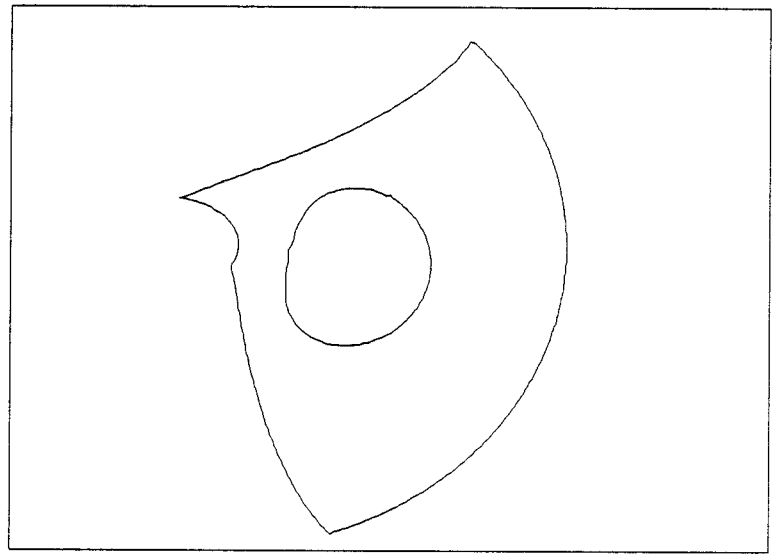

Fig. 5.5. An example of sub-space.

When a contour is presented, the whole area of this contour has to be examined again to determine whether or not a sub-space exists.

6. PARAMETER SELECTION AND BODY RANGE OF MOTION ANALYSIS

6.1. Selections of changes in leg segment parameters

The boundary for the body range of motion is a continuous surface but much of this boundary is of little interest since we are only concerned with walking. Only three horizontal plane sections of the boundary are determined. The heights of these curves have been selected to include the most likely walking height (Baek,1990).

Tables 2.1 to 2.6 show that coxa length for all legs is small (less than 1.35 mm) and absolute value of coxa twist is near 100 degrees (within 1.4 degrees). From the point of view of design and manufacturing of walking machines, one wonders why these lengths are not zero and angles not 90 degrees. Therefore, one set of simulations was done changing all coxa lengths, first to zero and then to twice their original lengths. Another set of simulations was done changing all coxa twists, first to 90 degrees and then to original angles increased by 10 degrees.

Finally, effects of changes in directions of body-coxa joint axes were examined. A set of simulations was done leaving the z-component of the body-coxa joint axis unit vector the same but changing the other components

(changing azimuth). First the y-component was made zero (direction 1) (i.e., direction set 1 in Fig. 6.1). This results in rotating the body-coxa axis of each leg about a line parallel to the body z-axis. Then the body-coxa axis of each leg was rotated by the same angle but in the opposite direction (direction 2).

A set of simulations was also done changing the z-component of the body-coxa joint axis unit vector (changing elevation) but leaving the other components unchanged. First the body-coxa axis for each leg was made parallel to the body z-axis (direction 5) (i.e. direction set 5 in Fig. 6.2); this results in rotating

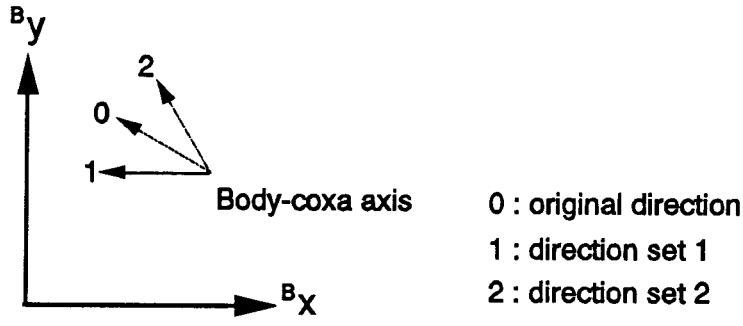

Fig. 6.1. Relationship among directions of body-coxa joint axes for sets 1,2 and original.

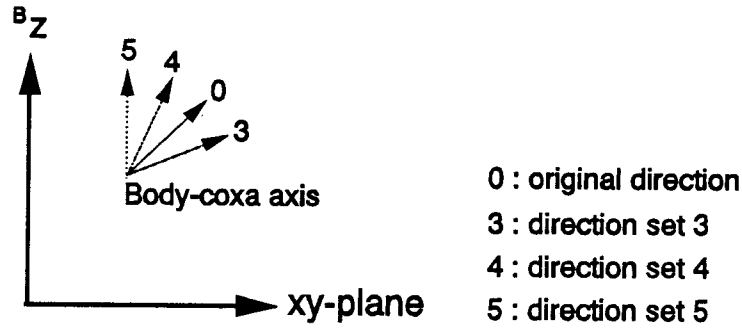

Fig. 6.2. Relationship among directions of body-coxa joint axes for sets 3, 4, 5 and original.

the body-coxa axis of each leg about a line parallel to the body xy-plane. Next each body-coxa axis was rotated in the same direction but through half the original angle (direction 4). Last, each body-coxa axis was rotated in the opposite direction through half the original angle (direction 3).

The beetle normally stands with its center-of-mass 10 mm above the ground and with the body xy-plane parallel to the ground. The effects of changes in the height have been evaluated by determining motion with center-of-mass at 8, 10 and 12 mm above the ground. The body ranges of motion are all determined with six feet fixed on the ground. Foot positions are determined by

finding center of foot range of motion for each height of center-of-mass.

6.2. Determination of foot positions for finding body range of motion with changed leg segment parameters

The body range of motion is found with six feet fixed on the ground. Foo (1991) showed that maximum body range of motion is with each foot at the center of the foot range of motion. Thus, center of foot range of motion used as foot position.

The computer program was prepared to determine body range of motion but it assumes a fixed body orientation and it can be constrained by any number of legs. Thus, foot range of motion can be determined by constraining body with only one leg. Foot range of motion determined in this way must be rotated and translated to the correct position for each foot. The following figures (Figs. 6.3 to 6.5) show foot ranges of motion for only right front, left middle and right hind legs; the others are symmetrical about the y-axis (${}^{B}y$). Histograms of stride length for each leg were plotted from foot ranges of motion.

The stride length histogram is drawn by calculating stride length at 1 mm interval along the x-axis from the foot range of motion (Figs. 6.3 to 6.5). From the three

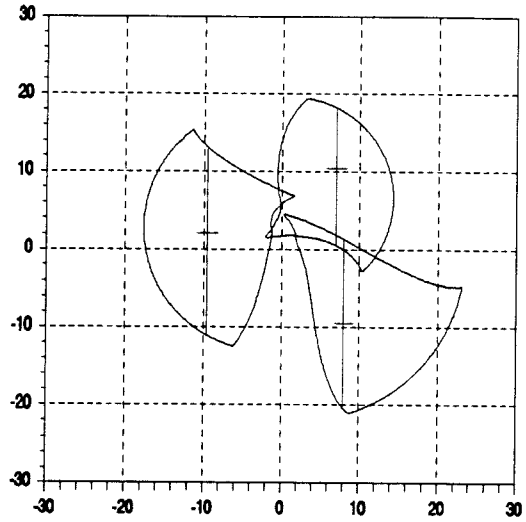

Foot ranges for right front, left middle and right hind legs at ^{B}z= 8 mm

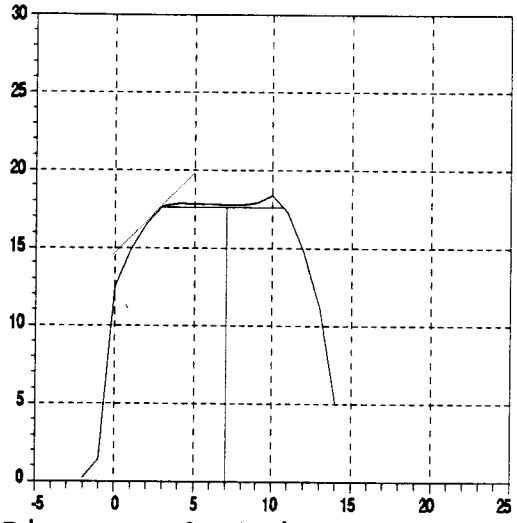

Diagram of stride length for right front leg at ^{B}z = 8 mm

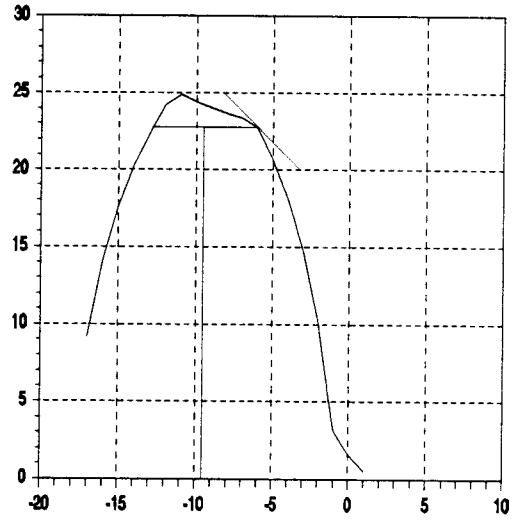

Diagram of stride length for left middle leg at ^{B}z = 8 mm

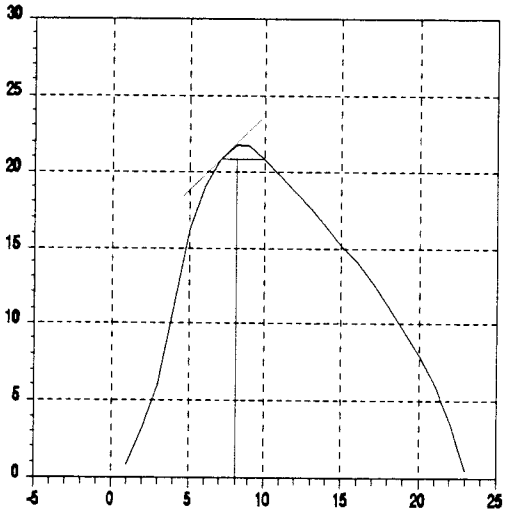

Diagram of stride length for right hind leg at ^{B}z = 8 mm

Fig. 6.3. Foot ranges and stride length diagrams for original leg parameters at ^{B}z = 8 mm. Dotted lines present procedure for determining foot positions.

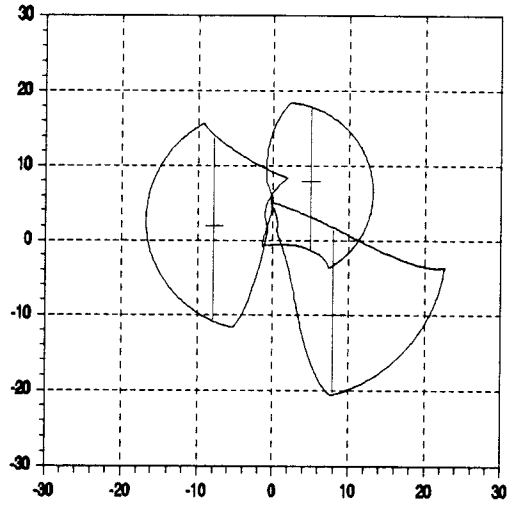

Foot ranges for right front, left middle and right hind legs at ^{B}z= 10 mm

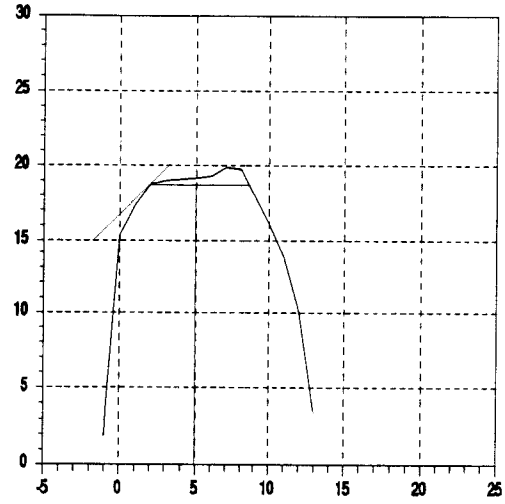

Diagram of stride length for right front leg at ^{B}z = 10 mm

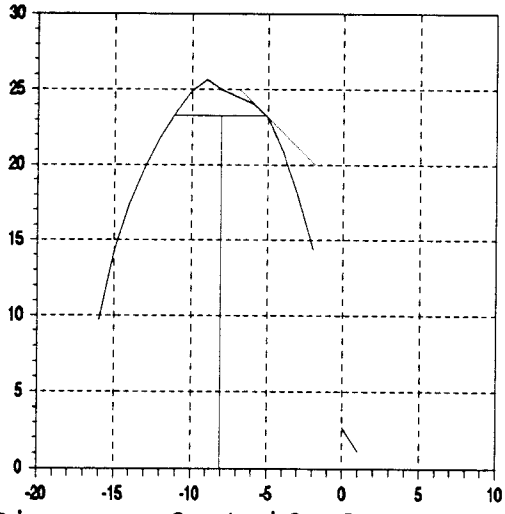

Diagram of stride length for left middle leg at ^{B}z = 10 mm

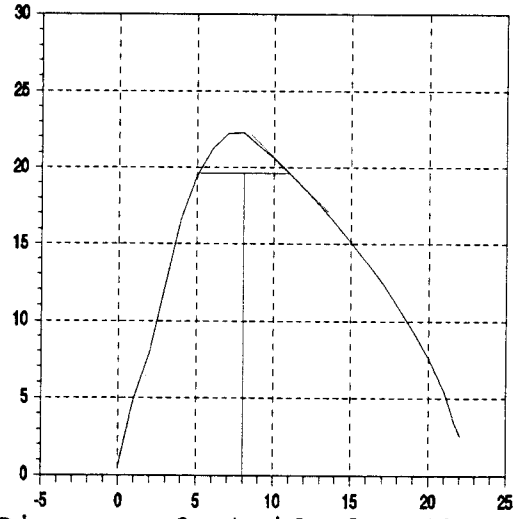

Diagram of stride length for right hind leg at ^{B}z = 10 mm

Fig. 6.4. Foot ranges and stride length diagrams for original leg parameters at ^{B}z = 10 mm. Dotted lines present procedure for determining foot positions.

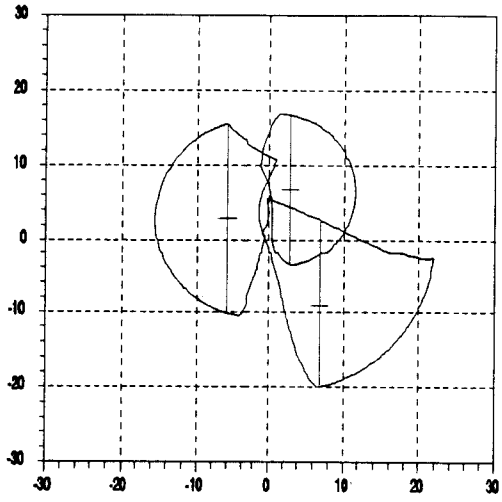

Foot ranges for right front, left middle and right hind legs at ^{B}z= 12 mm

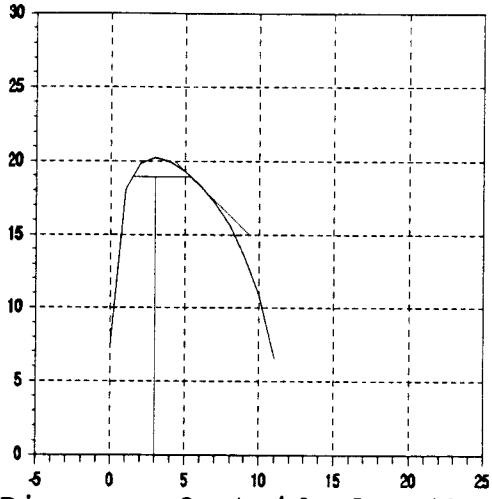

Diagram of stride length for right front leg at ^{B}z = 12 mm

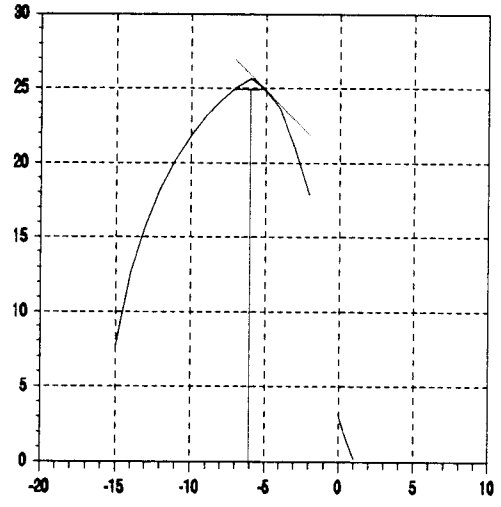

Diagram of stride length for left middle leg at ^{B}z = 12 mm

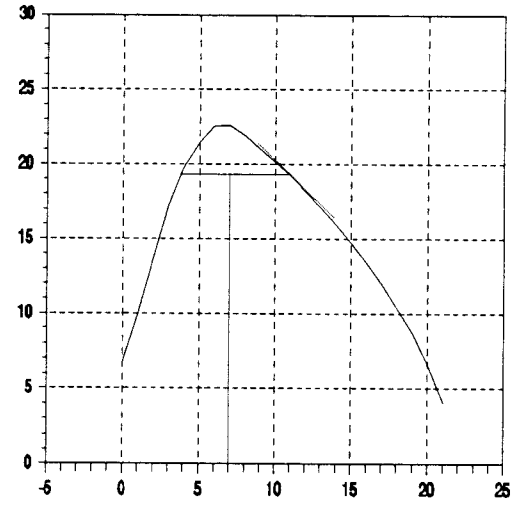

Diagram of stride length for right hind leg at ^{B}z = 12 mm

Fig. 6.5. Foot ranges and stride length diagrams for original leg parameters at ^{B}z = 12 mm. Dotted lines present procedure for determining foot positions.

figures, the diagrams of stride length for right front leg have a almost flat top. In Figs. 6.4 and 6.5, the stride length diagrams for left middle legs are discontinuous because the stride length is not calculated if the line along which stride length is measured in these cuts the foot range of motion more than twice.

Best foot positions (i.e., the center of foot range of motion) can be found from foot ranges of motion and stride length diagrams. First, a point's slope at 45 degrees can be found from the stride length diagram of every leg and the x- and y-coordinates of this point can be measured. A line, from edge to edge, can be plotted horizontally based on the y-coordinate of above point in each stride length diagram and a middle point of this segment can be measured. Then a vertical line can be plotted on respective foot range of motion according to the x-coordinate of this middle point. Along this vertical line, a middle point can be determined between two edges of respective foot range. This middle point is the foot position of each leg. This procedure is shown by dotted lines in Figs. 6.3 to 6.5 for different sets of foot positions. From the above procedure, foot positions of right front, left middle and right hind legs can be determined. The other foot positions of three legs can be found based on the leg's symmetry about ^{B}y axis. All sets of foot positions used in this study are listed in

appendix from tables A.1 to A.10 and only foot positions of right side legs are listed.

7. DISCUSSION

7.1. Effects of changing leg segment parameters on body and foot ranges of motion

In this chapter, body and foot ranges of motion are discussed with roll, pitch and yaw all equal to zero. Ranges are separated into four groups: coxa length, coxa twist, direction sets 1 and 2 and direction sets 3, 4 and 5 which are also compared with the comparable original parameter set for 8 , 10 and 12 mm heights. The square dots represent foot positions in the figures of body ranges; foot ranges show only right front, left middle and right hind legs. Figs. 7.1 and 7.2 show the real scales used for each of the component grid panels in Figs. 7.3 to 7.10. In both Figs. 7.1 and 7.2, the x and y axes are, respectively, the x-axis (^{B}x) and y-axis (^{B}y) of the body coordinate system.

Figs. 7.3 to 7.6 present the body ranges of motion. Based on these figures the following observations are made.

1) The centroid of foot positions is always within 0.6 mm of the origin.

2) When coxa length is twice original length ($2a_1$) range is largest of the group in Fig 7.3. Body ranges with a_1 = 0 and doubling a_1 are wider at height 8.

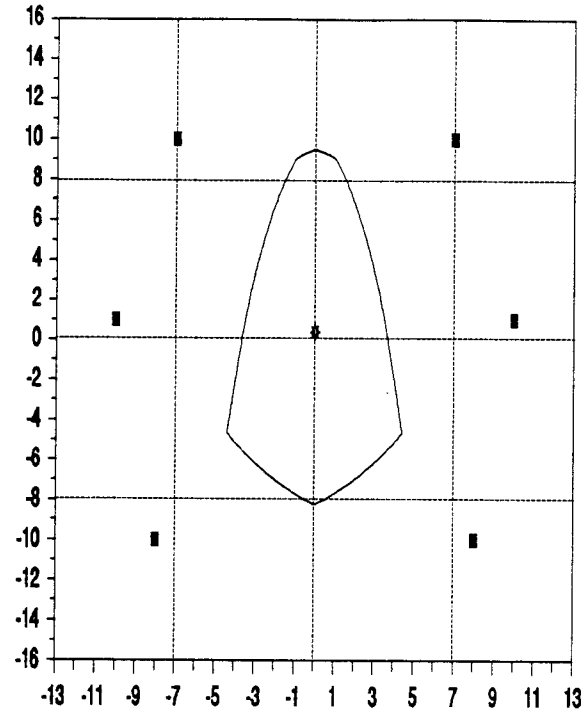

Fig. 7.1. Scale used in each body range of motion. The square blocks present the foot positions used in each case. "*" indicates centroid of foot positions.

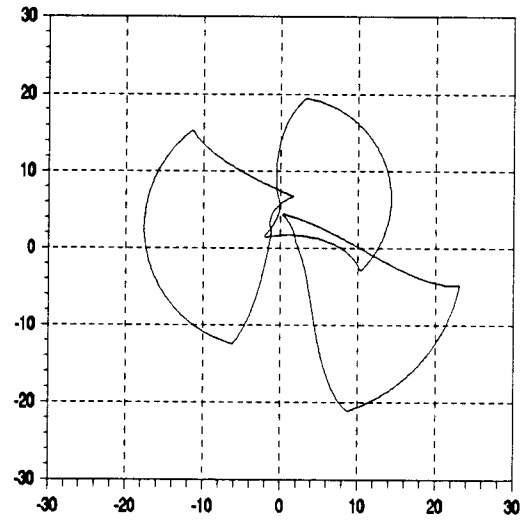

Fig. 7.2. Scale used in each foot range of motion.

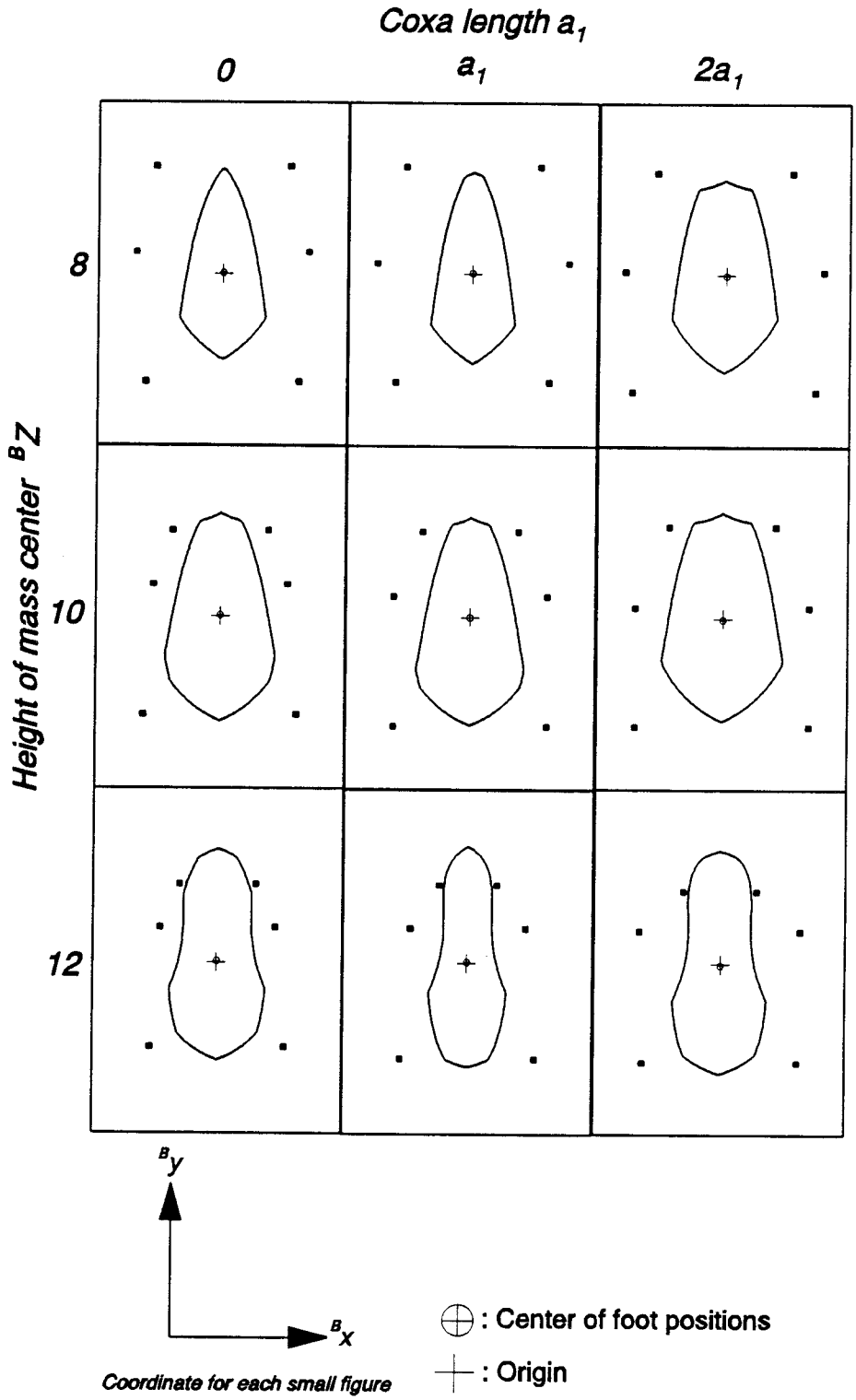

Fig. 7.3. Body ranges of motion for coxa lengths 0, a_1 and $2a_1$ at ^BZ = 8, 10 and 12 mm.

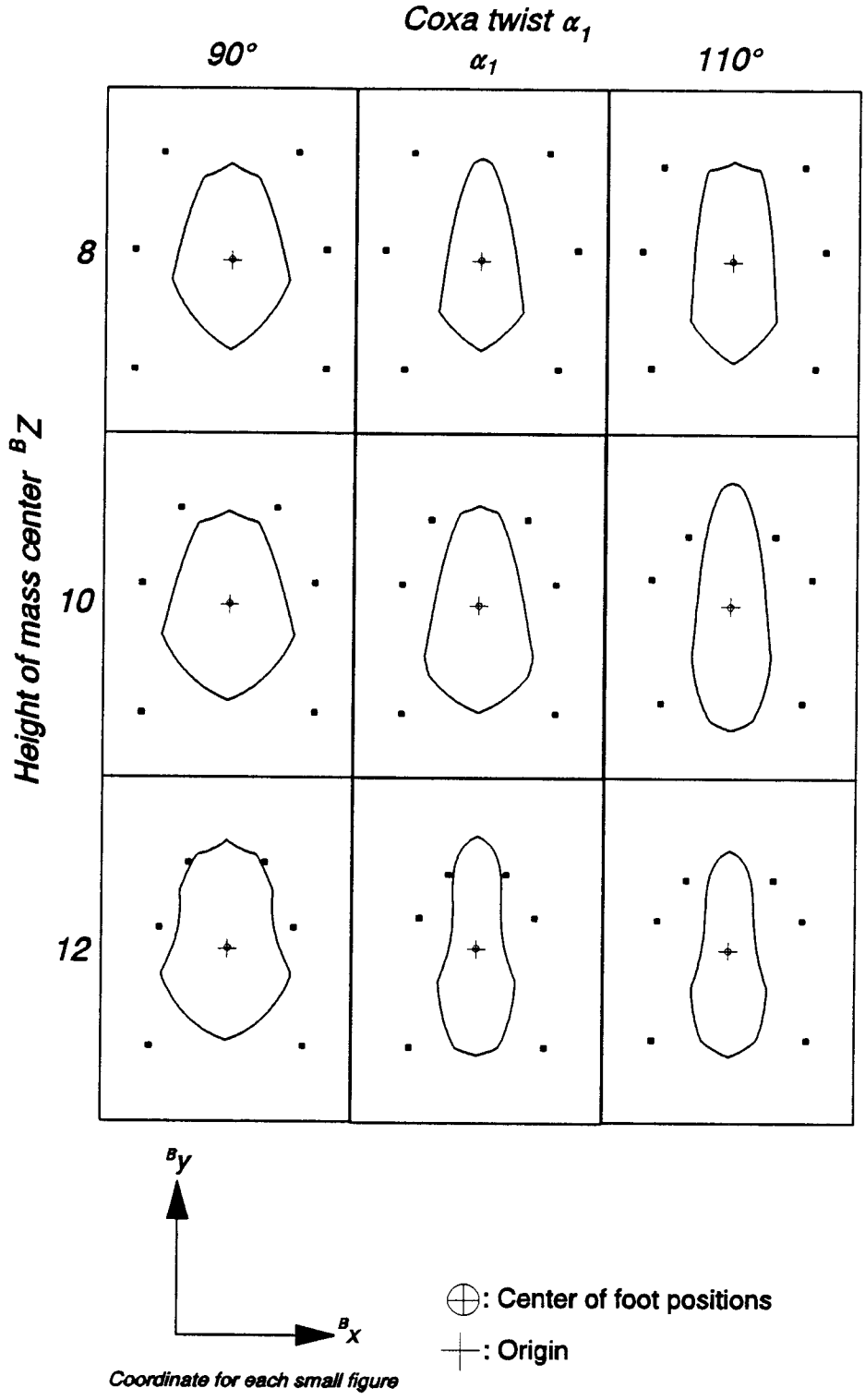

Fig. 7.4. Body ranges of motion for coxa twists 90°, α_1 and 110° at ^BZ = 8, 10 and 12 mm.

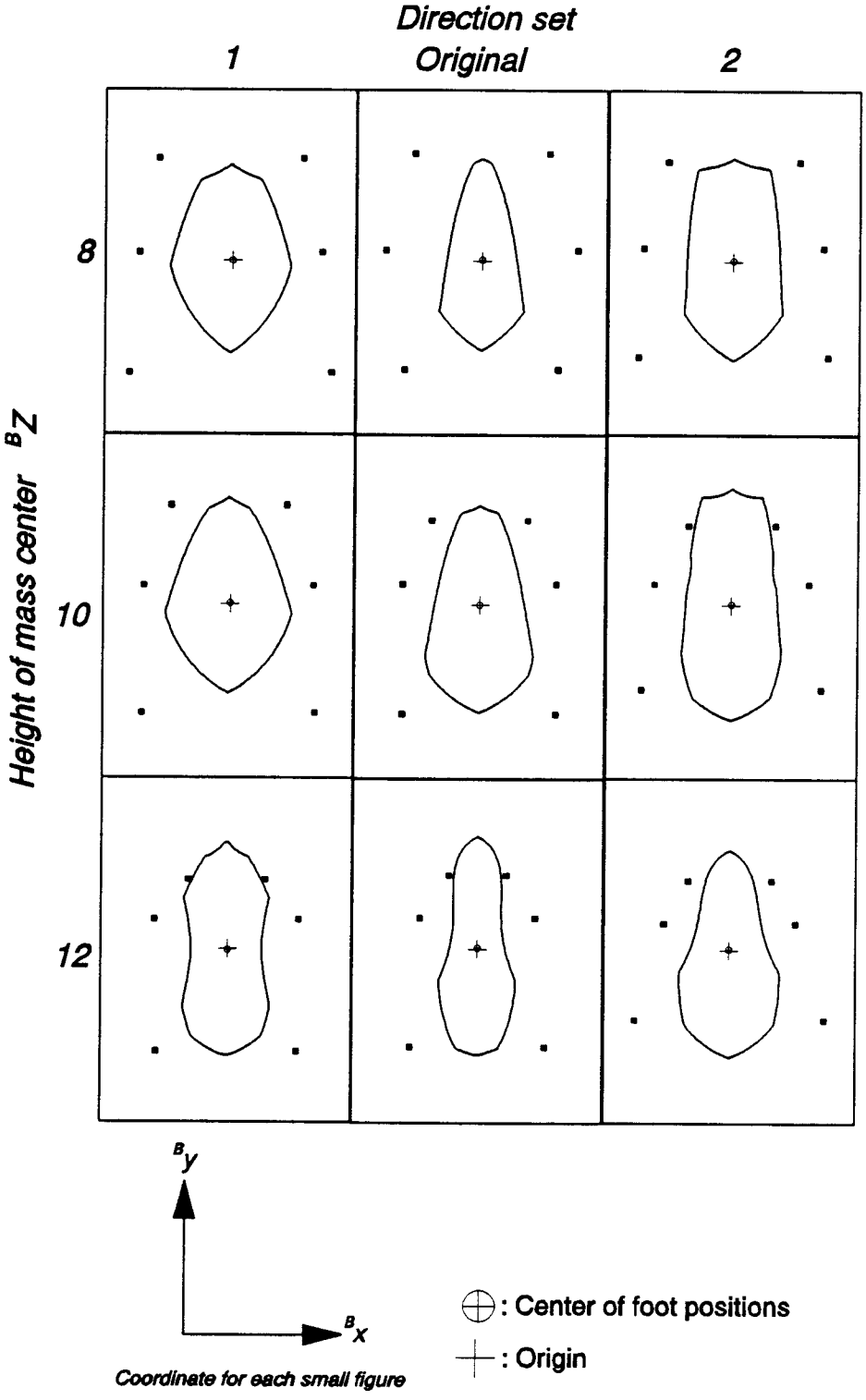

Fig. 7.5. Body ranges for changing body-coxa axis azimuth. Direction set 1 has zero y-component.

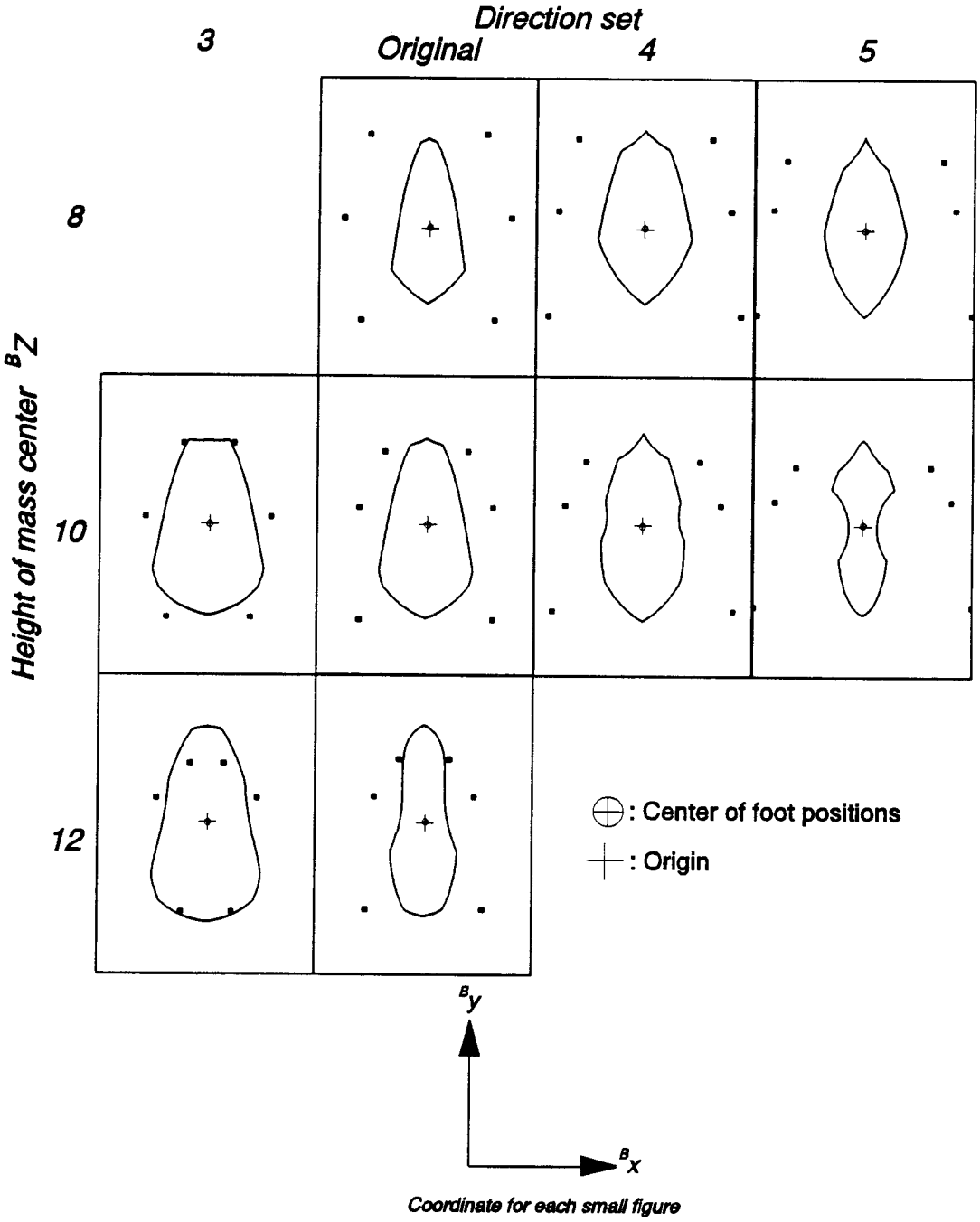

Fig. 7.6. Body ranges for changing body-coxa axis elevation. Direction set 5 makes axis vertical (z-component = -1).

3) When coxa twist (α_1) is 90° the ranges of motion are wider and shorter. If α_1 is 110°, the ranges are narrower and are shifted backward relative to the front feet.

4) Direction set 1 (Fig. 7.5) ranges are wider but shorter than original. Direction set 2 is longer (except ${}^{B}Z$ = 12 mm) and is shifted backward. These effects are similar to those of changing of coxa twist.

5) In Fig. 7.6, direction set 3 shows only case where feet are inside body range of motion. For direction set 5 feet are so far out to the side (Fig. 7.10) that body range of motion is very restricted.

Foot ranges of motion for each of these variations are shown in Figs. 7.7 to 7.10.

1) The front leg's foot range is not noticeably influenced changes in coxa length (Fig. 7.7).

2) If coxa length is zero, then ranges for middle and hind legs are shifted toward center and area is decreased. On the other hand, if coxa length is double, then these effects are reversed.

3) In Fig. 7.8, all three foot ranges of motion shift closer to center for 90° coxa twist and farther from center for 110° twist.

4) As azimuths of body-coxa joint axes rotated from direction set 1 (parallel to body zx-plane) through the original azimuth to direction set 2 the extent of foot

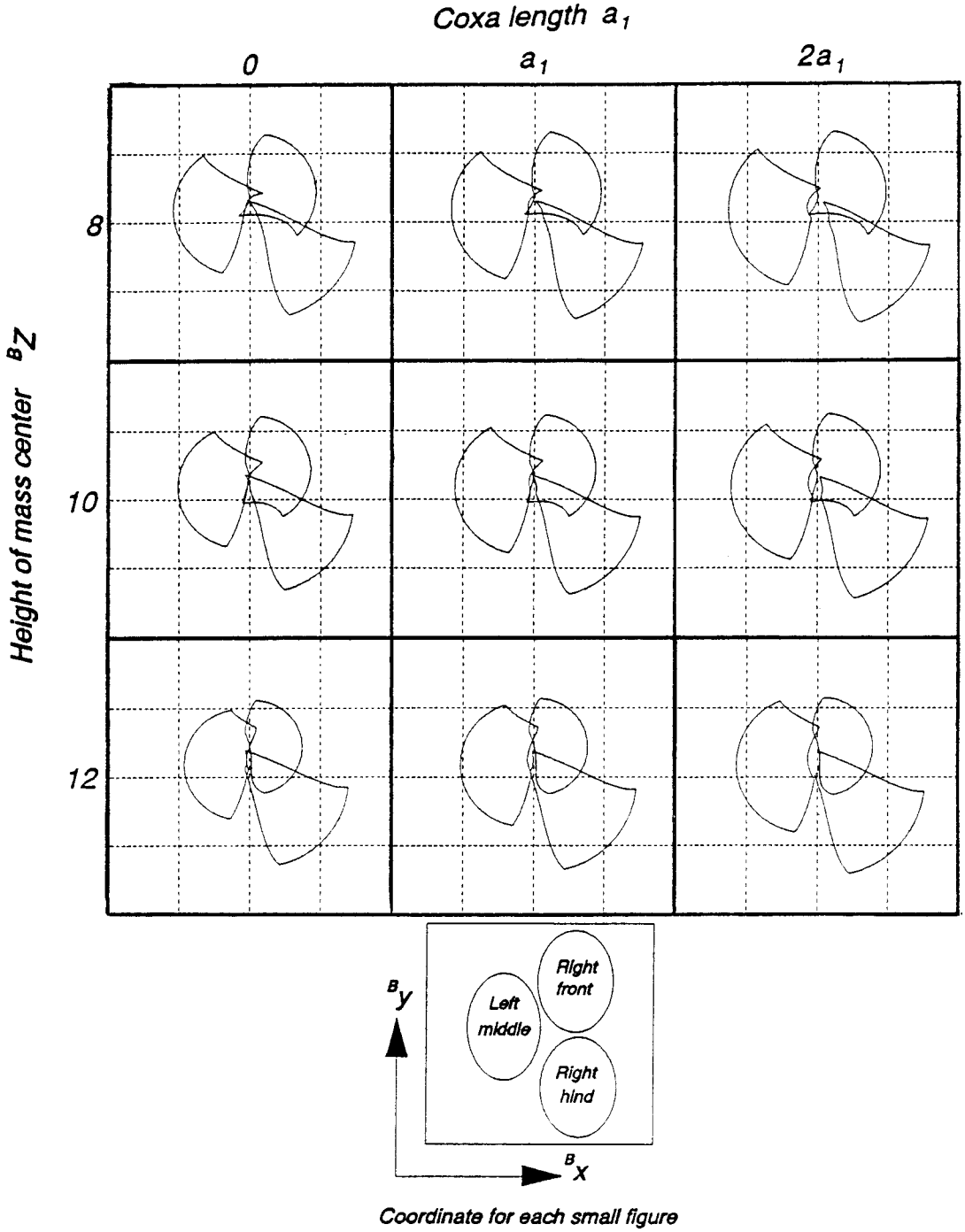

Fig. 7.7. Foot ranges of motion for coxa lengths 0, a_1 and $2a_1$ at ^BZ = 8, 10 and 12 mm.

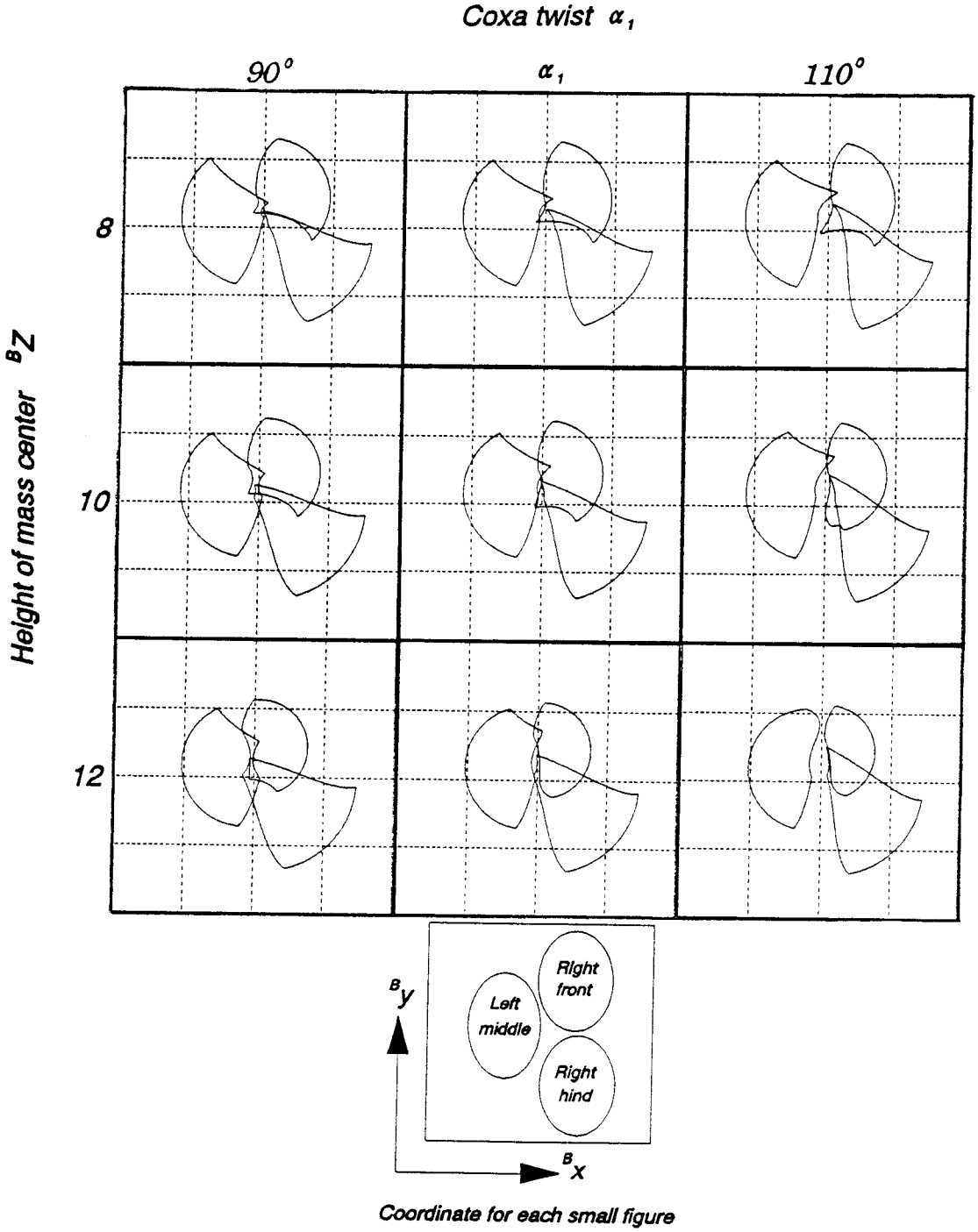

Fig. 7.8. Foot ranges of motion for coxa twists 90°, α_1 and 110° at ^BZ = 8, 10 and 12 mm.

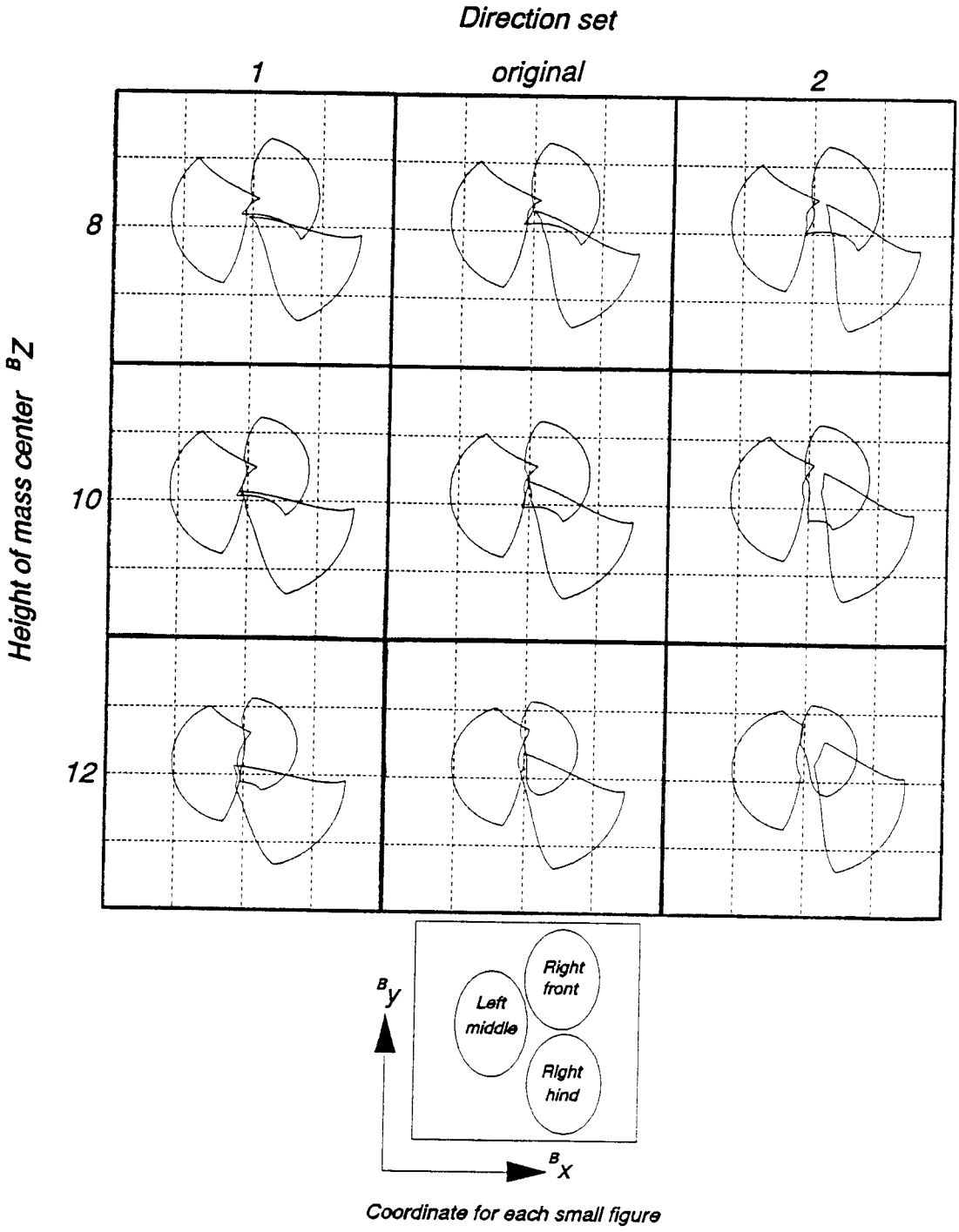

Fig. 7.9. Foot ranges for changing body-coxa axis azimuth. Direction set 1 has zero y-component.

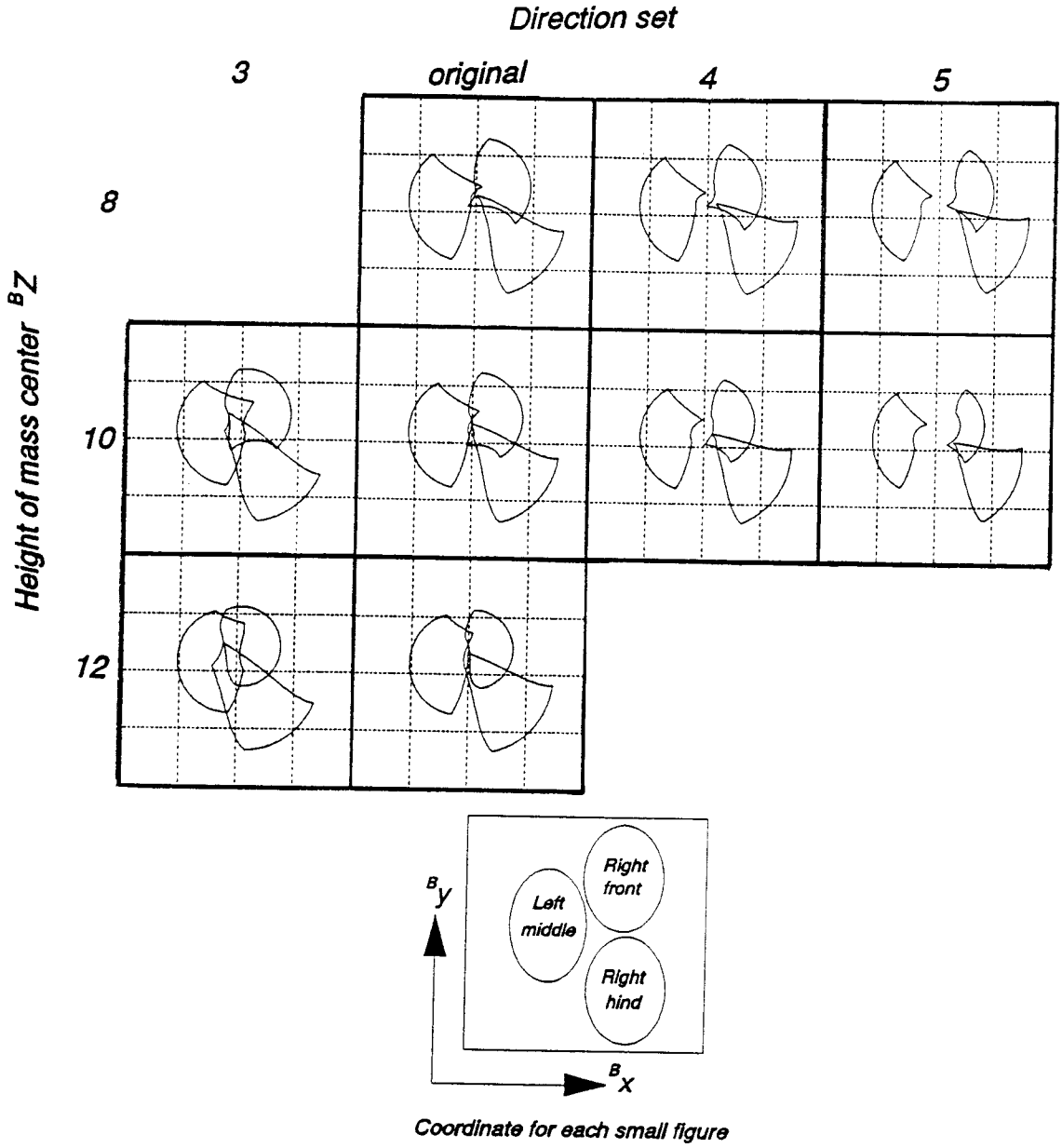

Fig. 7.10. Foot ranges for changing body-coxa axis elevation. Direction set 5 makes axis vertical (z-component = -1).

ranges in x direction decreases and extent in y direction increases.

5) As elevations of body-coxa joint axes rotated from direction set 5 (parallel to body xy-plane), 4 through the original direction to direction set 3 the foot ranges are closer to body y-axis and the extent of foot ranges in x and y directions increase.

7.2. Effects of changing leg segment parameters on pitch, roll and yaw ranges

For all body ranges of motion, until now, pitch, roll and yaw have all been equal to zero. Since pitch, roll and yaw do influence body range of motion their effect is consider here. However a full evaluation of their influence is not attempted but only coxa length zero is compared with original parameters as shown in tables 7.1 to 7.6. Both foot positions and body are symmetrical about the ^{B}y axis; therefore, the results are symmetrical about ^{B}y-axis and only left side data is shown in the tables. Each cell of these tables contains degrees range of roll, pitch or yaw located at top of cell and middle of range located at bottom.

From these tables, it is clear that there are substantial differences in orientation capability with change of coxa length. Therefore orientation capability

should be examined for other parameter changes.

Table 7.1. Degrees range and middle of range of pitch, rotation about x- axis, for original data.

^{B}y	^{B}z = 8 mm				^{B}z = 10 mm			^{B}z = 12 mm		
12	--- ---	--- ---	--- ---	27 -41.5	--- ---	--- ---	1 -17.5	--- ---	--- ---	--- ---
10	--- ---	48 -48	56 -38	61 -34.5	--- ---	62 -37	71 -38.5	--- ---	44 -36	68 -30
8	4 -38	44 -36	50 -28	59 -22.5	55 -36.5	73 -35.5	79 -32.5	--- ---	71 -33.5	81 -29.5
6	9 -27.5	36 -29	43 -20.5	54 -14	49 -29.5	67 -27.5	79 -22.5	--- ---	70 -28	83 -24.5
4	5 -24.5	32 -24	41 -15.5	54 -8	43 -23.5	62 -21	76 -15	--- ---	65 -21.5	81 -17.5
2	3 -22.5	30 -21	41 -11.5	57 -2.5	40 -19	62 -16	78 -9	--- ---	54 -18	79 -9.5
0	--- ---	32 -20	46 -9	64 1	37 -13.5	65 -11.5	82 -4	4 -10	43 -13.5	65 -6.5
-2	--- ---	28 -15	55 -7.5	78 4	35 -8.5	61 -3.5	84 3	4 -4	35 -8.5	51 -4.5
-4	--- ---	25 -9.5	59 -2.5	77 0.5	33 -2.5	53 3.5	64 4	--- ---	28 -4	40 -2
-6	--- ---	--- ---	35 -2.5	53 0.5	24 2	39 5.5	47 5.5	--- ---	20 -1	29 0.5
-8	--- ---	--- ---	--- ---	21 -4.5	--- ---	18 2	31 4.5	--- ---	12 1	19 1.5
-10	--- ---	--- ---	--- ---	--- ---	--- ---	--- ---	1 -4.5	--- ---	--- ---	0 -4
^{B}x	-6	-4	-2	0	-4	-2	0	-4	-2	0

Table 7.2. Degrees range and middle of range of pitch, rotation about x-axis, for coxa length = 0.

^{B}y	^{B}z = 8 mm				^{B}z = 10 mm			^{B}z = 12 mm		
12	--- ---	--- ---	--- ---	--- ---	--- ---	--- ---	0 -13	--- ---	--- ---	--- ---
10	--- ---	0 -26	54 -40	64 -34	0 -20	69 -39.5	77 -40.5	--- ---	58 -33	70 -34
8	4 -38	45 -36.5	50 -29	59 -23.5	56 -36	74 -35	81 -32.5	35 -45.5	70 -32	82 -28
6	9 -27.5	37 -29.5	44 -21	55 -15.5	50 -29	70 -27	82 -22	34 -36	69 -26.5	84 -22
4	5 -24.5	33 -24.5	41 -15.5	55 -8.5	45 -22.5	67 -20.5	80 -14	33 -28.5	69 -20.5	84 -16
2	2 -22	32 -21	43 -11.5	59 -3.5	42 -17	66 -15	83 -7.5	31 -21.5	64 -13	83 -8.5
0	--- ---	33 -18.5	48 -9	67 0.5	40 -12	62 -7	85 -0.5	30 -15	54 -9	70 -5
-2	--- ---	29 -13.5	58 -8	80 4	35 -4.5	58 2	75 5.5	26 -10	43 -5.5	56 -3
-4	--- ---	23 -6.5	52 2	68 4	32 3	47 6.5	57 6.5	21 -4.5	33 -2.5	44 -1
-6	--- ---	--- ---	25 -0.5	44 3	16 3	32 7	41 7.5	14 -1	24 0	33 0.5
-8	--- ---	--- ---	--- ---	9 -5.5	--- ---	11 2.5	25 5.5	--- ---	9 -1.5	20 0
^{B}x	-6	-4	-2	0	-4	-2	0	-4	-2	0

Table 7.3. Degrees range and middle of range of roll, rotation about y-axis, for original data.

^{B}y	^{B}z = 8 mm				^{B}z = 10 mm					^{B}z = 12 mm				
10	-- --	-- --	-- --	-- --	-- --	-- --	-- --	-- --	-- --	-- --	-- --	-- --	2 -5	6 0
8	-- --	-- --	8 -11	26 0	-- --	-- --	0 14	14 -6	30 0	-- --	-- --	6 -12	14 -6	16 0
6	-- --	20 -32	35 -15.5	38 0	-- --	11 -27.5	27 -20.5	37 -11.5	40 0	-- --	2 -19	11 -13.5	18 7	20 0
4	5 -41.5	25 -25.5	41 -13.5	48 0	-- --	18 -26	33 -18.5	43 -10.5	48 0	-- --	5 -20.5	13 -14.5	19 -7.5	20 0
2	10 -35	25 -20.5	41 -8.5	54 0	8 -29	24 -25	37 -17.5	48 -9	52 0	-- --	8 -21	15 -14.5	20 -8	22 0
0	13 -31.5	27 -17.5	42 -6	52 0	12 -28	29 -23.5	42 -17	53 -8.5	58 0	-- --	10 -21	18 -15	23 -7.5	24 0
-2	17 -29.5	30 -16	45 -4.5	52 0	-- --	31 -22.5	45 -15.5	56 -8	62 0	1 -24.5	14 -20	24 -14	29 -7.5	30 0
-4	-- --	35 -15.5	49 -4.5	58 0	-- --	33 -20.5	48 -14	56 -8	60 0	-- --	17 -18.5	26 -14	33 -7.5	36 0
-6	-- --	-- --	58 -6	68 0	-- --	-- --	45 -15.5	53 -8.5	56 0	-- --	12 -18	24 -15	31 -8.5	32 0
-8	-- --	-- --	-- --	36 0	-- --	-- --	-- --	44 -9	46 0	-- --	-- --	4 -8	23 -8.5	24 0
^{B}x	-6	-4	-2	0	-8	-6	-4	-2	0	-8	-6	-4	-2	0

Table 7.4. Degrees range and middle of range of roll, rotation about y-axis, for coxa length $a_1 = 0$.

${}^{B}y$	${}^{B}z$ = 8 mm				${}^{B}z$ = 10 mm					${}^{B}z$ = 12 mm			
10	-- --	-- --	-- --	-- --	-- --	-- --	-- --	-- --	-- --	-- --	-- --	-- --	8 0
8	-- --	-- --	8 -13	24 0	-- --	-- --	7 -14.5	20 -6	32 0	-- --	-- --	18 -5	22 0
6	-- --	18 -32	33 -15.5	38 0	-- --	14 -26	29 -19.5	41 -11.5	42 0	-- --	16 -11	24 -6	26 0
4	7 -41.5	32 -29	44 -14	48 0	-- --	21 -24.5	35 -17.5	45 -9.5	50 0	9 -17.5	19 -12.5	25 -6.5	28 0
2	17 -37.5	34 -24	48 -12	56 0	10 -28	27 -23.5	39 -16.5	50 -8	54 0	12 -18	22 -13	27 -6.5	30 0
0	23 -34.5	36 -21	51 -9.5	62 0	12 -26	31 -22.5	44 -16	54 -8	60 0	16 -18	25 -12.5	31 -6.5	32 0
-2	26 -32	42 -20	55 -8.5	66 0	-- --	34 -21	48 -15	58 -8	62 0	19 -16.5	30 -12	36 -6	38 0
-4	-- --	50 -21	63 -9.5	72 0	-- --	35 -19.5	48 -15	58 -9	60 0	19 -15.5	31 -11.5	39 -6.5	42 0
-6	-- --	-- --	67 -9.5	74 0	-- --	-- --	44 -16	52 -9	54 0	-- --	26 -12	37 -7.5	38 0
-8	-- --	-- --	-- --	-- --	-- --	-- --	-- --	41 -9.5	42 0	-- --	-- --	29 -7.5	32 0
${}^{B}x$	-6	-4	-2	0	-8	-6	-4	-2	0	-6	-4	-2	0

Table 7.5. Degrees range and middle of range of yaw, rotation about z-axis, for original data.

^{B}y	^{B}z = 8 mm			^{B}z = 10 mm			^{B}z = 12 mm		
10	--- ---	--- ---	--- ---	--- ---	--- ---	--- ---	--- ---	--- ---	6 0
8	--- ---	6 5	6 0	8 9	10 5	10 0	--- ---	12 5	12 0
6	10 11	12 6	12 0	15 10.5	17 5.5	18 0	--- ---	20 6	20 0
4	15 12.5	18 6	18 0	16 9	24 6	24 0	--- ---	16 1	28 0
2	20 14	24 7	26 0	13 5.5	31 6.5	32 0	--- ---	17 -2.5	38 0
0	17 10.5	32 8	34 0	16 5	40 7	42 0	--- ---	23 -4.5	48 0
-2	14 8	35 5.5	42 0	18 2	39 1.5	54 0	7 -6.5	32 -6	46 0
-4	10 3	35 0.5	48 0	20 -2	41 -3.5	50 0	17 -9.5	36 -9	38 0
-6	--- ---	31 -4.5	38 0	20 -5	35 -5.5	38 0	15 -10.5	28 -8	28 0
-8	--- ---	--- ---	10 0	0 -7	22 -3	28 0	4 -7	18 -7	20 0
^{B}x	-4	-2	0	-4	-2	0	-4	-2	0

Table 7.6. Degrees range and middle of range of yaw, rotation about z-axis, for coxa length $a_1 = 0$.

${}^{B}y$	${}^{B}z$ = 8 mm			${}^{B}z$ = 10 mm			${}^{B}z$ = 12 mm		
10	--- ---	--- ---	--- ---	--- ---	--- ---	--- ---	--- ---	--- ---	8 0
8	--- ---	5 4.5	6 0	20 10	12 5	12 0	--- ---	15 5.5	16 0
6	10 11	11 5.5	12 0	17 11.5	19 5.5	20 0	--- ---	22 6	24 0
4	15 12.5	18 6	18 0	18 9	27 6.5	28 0	--- ---	31 6.5	32 0
2	21 13.5	24 7	26 0	14 5	36 7	38 0	--- ---	31 2.5	44 0
0	17 10.5	32 8	34 0	18 4	42 5	48 0	8 -4	35 -1.5	56 0
-2	15 7.5	35 5.5	44 0	20 0	43 -0.5	60 0	18 -5	44 -5	58 0
-4	8 1	36 0	48 0	24 -5	42 -5	48 0	25 -8.5	45 -8.5	46 0
-6	--- ---	27 -5.5	36 0	15 -3.5	30 -3	38 0	14 -6	32 -6	36 0
-8	--- ---	--- ---	--- ---	--- ---	14 -1	22 0	--- ---	16 -2	24 0
${}^{B}x$	-4	-2	0	-4	-2	0	-4	-2	0

7.3. Effects of use of the numerical method

In this study, the Bairstow method, a numerical method, has been used to solve the quartic equations. The solutions obtained from the use of the Bairstow method are sufficiently close to real values. However, this method led to some inaccurate results. For example, the body range of motion in Fig. 7.11 has two flaws at the top of range where, from geometric reasoning, the range should be a smooth curve. After changing the constraint value used in the Bairstow method, the result was somewhat improved, but concave points remained at the same positions. During the process of solving with varying pitch, roll and yaw, a set of foot positions was used as a test of the computer program . After comparing the results of this test to those obtained by Foo (1991), there was a one degree of difference in some values. The Bairstow method worked reasonably well for all cases except these two.

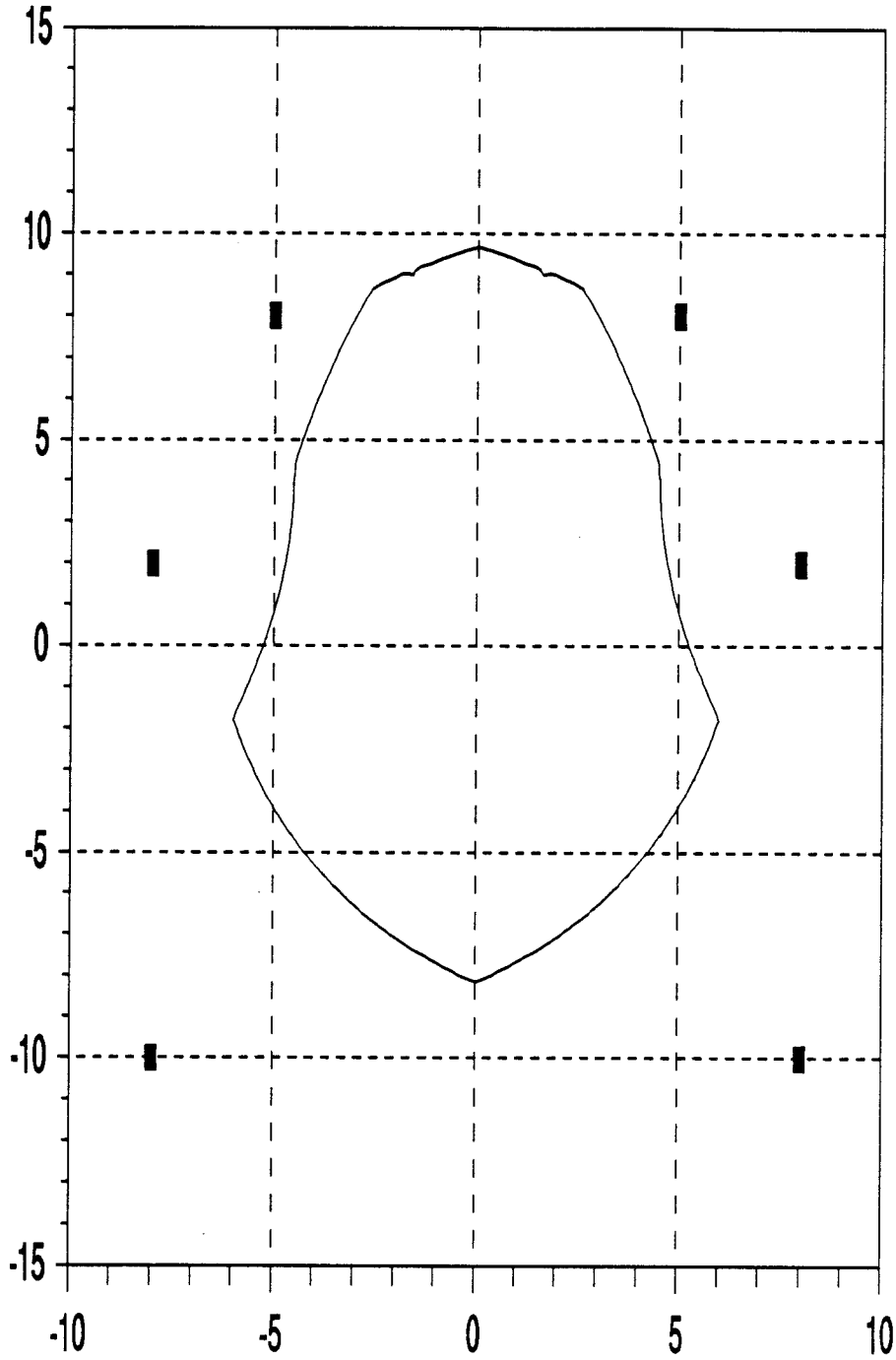

Fig. 7.11. An example of effect of Bairstow method. The black blocks present six foot positions. Two concave points are occurred around at (±2,9).

8.CONCLUSION

This study examined the effects on body range of motion of changed leg parameters. Results were obtained by comparing body ranges of motion for changed parameter sets with that of original parameter set. Foot ranges of motion were also examined to gain a better understanding of the effects of parameter changes.

Some conclusions are obvious when parameters were changed. Results of changing coxa twists and changing azimuth of body coxa axes are similar. Foot positions of direction set 3 are within body ranges of motion because foot ranges are much closer to ${}^{B}y$ axis. Another important observation is the nearness of centroid of foot positions and origin of ${}^{B}x$-${}^{B}y$ plane. Further studies are needed to fully investigate these phenomena.

In this study, leg parameters were changed for all six legs in each case. However, the study can be extended to observe effects of changing parameters for a pair of legs, with the other two pairs unchanged. For example, the front leg's foot ranges are not obviously influenced by changes in coxa length. Then, effects on body ranges of motion may be studied for changing coxa twists of front legs and changing coxa length of other legs.

Current study of body ranges of motion involves

symmetrical foot positions and does not consider pitch, roll and yaw. Future study considering pitch, roll and yaw and non-symmetrical foot positions can provide more information in design of walking machine.

Finally, this study of ranges of motion focuses on positioning problems of kinematics only. Statics of standing beetles also needs study.

BIBLIOGRAPHY

Baek, Y.S., 1990. Kinematic Analysis of Legged System Locomotion on Smooth Horizontal Surfaces. Ph.D. thesis, Oregon State University.

Booth, A.D. and Booth, K.H.V., 1965. Automatic Digital Calculators. Butterworths Scientific Publications, pp.197-203.

Bowden,B.V., 1953. Faster than Thought. Sir Isaac Pitman & Sons, Ltd., pp.203-209.

Cordray, R.E., 1957. Remarks on a Recent Paper. J. ACM, Oct., vol.4, No.4, pp. 524-529.

Craig, J.J., 1986. Introduction to Robotics. Addison Wesley, pp. 60-130.

Denavit, J. and Hartenberg, R.S., 1955. A Kinematic Notation for Lower-Pair Mechanisms Based on Matrices. J. of Applied Mechanics, June, vol.77, pp. 215-221.

Fichter, E.F., 1986. A stewart Platform-Based Manipulator: General Theory and Practical Construction. J. of Robotics Research, Summer, vol.5, No.2, pp. 157-182.

Fichter, E.F., Fichter, B.L. and Albright, S.L., 1987. Arthropods: 350 Million Years of Successful Walking Machine Design. Proceeding of the Seventh World Congress on the Theory of Machines and Mechanisms, Sevilla, Spain, September, pp. 1877-1880.

Fichter, E.F. and Fichter, B.L., 1988. A Survey of Legs of Insects and Spiders from a Kinematic Perspective. Proceedings of IEEE International Conference on Robotics and Automation, Philadelphia, PA, April, pp. 984-986.

Foo, C.K., 1991. Range of Motion of Beetle Body as a Function of Foot Positions. M.S. thesis, Oregon State University.

Gewecke, M. and Wendler, G., 1985. Insect Locomotion. Paul Parey, pp. 1-102.

Haberman, C.M., 1966. Use of Digital Computers for Engineering Applications. Charles E. Merrill Books, pp. 103-104.

Herriot, J.G., 1963. Methods of Mathematical Analysis and Computation. John Wiley & Sons, Inc., pp. 44-47.

King, J.T., 1984. Introduction to Numerical Computation. McGraw-Hill, Inc.

Mason, R.M., 1956. The Digital Approximation of Contours. J. ACM, Oct., vol.3, No.4, pp. 355-359.

Mason, R.M., 1957. Remarks on a Recent Paper. J. ACM, Oct., vol.4, No.4, pp. 524-529.

Pedley, T.J., 1977. Scale Effects in Animal Locomotion. Academic Press.

Press, W.H., Flannery, B.P., Teukolsky, S.A. and Vetterling, W.T., 1989. Numerical Recipes: The Art of Scientific Computing (FORTRAN Version). Cambridge University Press, pp.259-269.

Song, S.M. and Waldron, K.J., 1989. Machines That Walk. The MIT Press, pp. 1-4.

Snyder, W.E., 1985. Industrial Robots: Computer Interfacing and Control. Prentice-Hall, Inc.

Todd, D.J., 1985. Walking Machines: An Introduction to legged Robots. Chapman and Hall.

APPENDIX

Table A.1. Foot positions: original data.

^{B}z	right front		right middle		right hind	
	x	y	x	y	x	y
8	7.0	10.0	10.0	1.0	8.0	-10.0
10	5.0	8.0	8.0	2.0	8.0	-10.0
12	3.0	7.0	6.0	3.0	7.0	-9.0

Table A.2. Foot positions: coxa lengths $a_1 = 0$.

^{B}z	right front		right middle		right hind	
	x	y	x	y	x	y
8	7.0	10.0	9.0	2.0	8.0	-10.0
10	5.0	8.0	7.0	3.0	8.0	-9.0
12	4.0	7.0	6.0	3.0	7.0	-8.0

Table A.3. Foot positions: coxa lengths $a_1 = a_1 \times 2$.

^{B}z	right front		right middle		right hind	
	x	y	x	y	x	y
8	7.0	9.5	10.3	0.3	9.5	-10.8
10	5.5	8.5	9.0	1.0	9.0	-10.0
12	3.8	6.5	8.3	2.8	8.0	-9.3

Table A.4. Foot positions: coxa twists $\alpha_1 = 90°$.

^{B}z	right front		right middle		right hind	
	x	y	x	y	x	y
8	7.0	10.0	10.0	1.0	10.0	-10.0
10	5.0	9.0	9.0	2.0	9.0	-10.0
12	4.0	8.0	7.0	2.0	8.0	-9.0

Table A.5. Foot positions: coxa twists α_1 = 110°.

^Bz	right front		right middle		right hind	
	x	y	x	y	x	y
8	7.3	8.8	9.5	1.0	8.5	-9.8
10	4.5	6.5	8.3	2.5	7.3	-9.0
12	4.5	6.5	7.5	2.8	8.0	-8.3

Table A.6. Foot positions: direction set 1.

^Bz	right front		right middle		right hind	
	x	y	x	y	x	y
8	7.5	9.5	9.5	0.8	10.5	-10.3
10	6.0	9.3	8.8	1.8	9.0	-10.0
12	4.0	6.5	7.5	2.8	7.3	-9.5

Table A.7. Foot positions: direction set 2.

^Bz	right front		right middle		right hind	
	x	y	x	y	x	y
8	6.8	9.3	9.3	1.3	9.8	-8.8
10	4.5	7.5	8.0	2.0	9.3	-7.8
12	4.3	6.5	6.8	2.5	9.8	-6.5

Table A.8. Foot positions: direction set 3.

^Bz	right front		right middle		right hind	
	x	y	x	y	x	y
8	----	----	----	----	----	----
10	3.0	8.8	7.5	1.0	5.0	-9.8
12	2.0	6.5	6.0	2.8	3.0	-9.3

Table A.9. Foot positions: direction set 4.

${}^{B}z$	right front		right middle		right hind	
	x	y	x	y	x	y
8	8.0	9.5	10.3	1.8	11.5	-9.5
10	6.8	7.0	9.3	2.3	10.8	-9.0
12	----	----	----	----	----	----

Table A.10. Foot positions: direction set 5.

${}^{B}z$	right front		right middle		right hind	
	x	y	x	y	x	y
8	9.3	7.3	10.8	2.0	12.8	-9.3
10	8.0	6.5	10.5	2.8	13.0	-8.5
12	----	----	----	----	----	----